CRYSTAL DYNAMICS OF PLATINUM

CRYSTAL DYNAMICS OF PLATINUM

by

DAVID HAMILTON DUTTON B.Sc.

A Thesis

Submitted to the Faculty of Graduate Studies

in Partial Fulfilment of the Requirements

for the Degree

Master of Science

McMaster University

September 1970

MASTER OF SCIENCE (1970) McMASTER UNIVERSITY
(Physics) Hamilton, Ontario.

TITLE: The Crystal Dynamics of Platinum

AUTHOR: David Hamilton Dutton, B.Sc.(Bishop's University)

SUPERVISOR: Professor B.N. Brockhouse

NUMBER OF PAGES: viii, 68

SCOPE AND CONTENTS:

The dispersion relations in Platinum have been measured at 90°K by the inelastic scattering of thermal neutrons. Born-von Kármán models of the force system have been calculated by a process of linear least squares fitting to the dispersion curves. Fourth neighbour forces with weaker interactions extending to at least sixth neighbours are required to fit the data. A frequency distribution has been computed using the force constants of the most realistic model.

Some interesting anomalous behaviour in the [0ζζ]T_1 branches of both Platinum and Palladium has been investigated in detail at temperatures of 90,296 and 473°K. A qualitative analysis indicates that the behaviour is caused by the Kohn effect though its manifestation is rather unusual.

ACKNOWLEDGEMENTS

First I should like to extend my thanks to my research supervisor, Professor B.N. Brockhouse. His advice and instruction have been invaluable aids throughout this work.

I am indebted to the staff of Atomic Energy of Canada Limited for the use of their facilities. In particular may I thank the members of the Neutron Physics Group for their kind assistance and many helpful suggestions.

I should also like to thank my colleagues at McMaster University; Dr. A.P. Miiller, Mr. J.R.D. Copley, Mr. R.R. Dymond, Mr. W.A. Kamitakahara, Mr. A. Larose, Mr. A.P. Roy and Mr. H.C. Teh for their help in planning and executing the experiments. Mr. Copley's help with various computer programs is particularly appreciated. To Dr. A.P. Miiller (now at Brandon University) goes my gratitude for long hours spent discussing the problems considered in this thesis. The work described in Chapter III is a logical extension of Dr. Miiller's earlier work and the explanation of the observed phenomena is due to him.

I am grateful to the **National Research Council** for financial support in the form of a National Research

Council Scholarship. In addition the work was supported by National Research Council grants.

Finally, my thanks to Mrs. S. McQueen for her typing and to Mrs. S. Duke for drawing many of the diagrams.

TABLE OF CONTENTS

	Page
CHAPTER I - INTRODUCTION	1
1. Outline of Thesis	1
2. Lattice Dynamics: An Historical sketch	2
3. The Born-von Kármán Theory of Lattice Dynamics	6
4. Scattering of Neutrons from Single Crystals	14
CHAPTER II - THE LATTICE DYNAMICS OF PLATINUM	19
1. Introduction	19
2. Triple Axis Spectrometer	19
3. Experimental Results	23
4. Discussion and Analysis of Results	29
CHAPTER III - ANOMALOUS LATTICE VIBRATIONS IN PLATINUM AND PALLADIUM	43
1. Introduction	43
2. The Kohn Effect	44
3. Experimental Results	46
4. Discussion and Analysis of Results	57
APPENDIX I - NUMERICAL FREQUENCY DISTRIBUTION OF PLATINUM	65
BIBLIOGRAPHY	66

LIST OF FIGURES

		Page
Figure I-1.	The (100) and (1$\bar{1}$0) planes of the reciprocal lattice of an f.c.c. lattice showing the boundaries of the first Brillouin zones.	12
Figure II-1.	Schematic diagram of the McMaster University Triple Axis Spectrometer.	21
Figure II-2.	Representative neutron groups from each of the branches of the dispersion curves of Platinum.	26
Figure II-3.	The dispersion curves of Platinum at 90°K.	28
Figure II-4.	The fitting error of a Born von-Kármán model as a function of the number of neighbours included in the model.	31
Figure II-5.	The distribution of frequencies in Platinum at 90°K calculated from a six neighbour Born von-Kármán model.	36
Figure II-6.	The lattice specific heat of Platinum calculated from the frequency distribution of Fig. II-5.	39
Figure III-1.	The T_1 branches of Palladium and Platinum.	48
Figure III-2.	The temperature dependence of the T_1 branch of Platinum.	50
Figure III-3.	The T_1 branch of Palladium comparing the results of Miiller to those of the present work.	52
Figure III-4.	The slopes of the transverse branches in the (100) plane of Platinum at angles of 7.5,15.0, 22.5,and 30.0° to the [110] direction.	54

		Page
Figure III-5.	The T_2 branch of Palladium at 90°K.	55
Figure III-6.	The T_1 branch of Nickel at 90°K.	56
Figure III-7.	Cross sections of the Fermi surfaces of Palladium and Platinum in both the (100) and (1$\bar{1}$0) planes.	59
Figure III-8.	One Quarter of the first Brillouin zone in the (100) plane of Platinum showing Kohn anomaly surfaces.	61
Figure III-9.	One quarter of the first Brillouin zone in the (100) plane of Palladium showing Kohn anomaly surfaces.	62

LIST OF TABLES

		Page
Table II-1.	The various incident energies used in the experiment are given here, in units of energy, frequency, and wavelength.	24
Table II-2.	Normal mode frequencies for Platinum at 90°K.	27
Table II-3.	Atomic force constants for three Born-von Kárman models of Platinum.	33
Table II-4.	A comparison of atomic force constants in Pt,Pd,Ag,Cu and Ni.	34
Table II-5.	Atomic force constants for Platinum when the anomalous T_1 branch is replaced by a smooth curve.	41
Table III-1.	Normal mode frequencies in the T_1 branch of Platinum at 90,296 and 473°K.	47
Table III-2.	Normal mode frequencies in off-symmetry directions in the (100) plane of Palladium.	53

CHAPTER I

INTRODUCTION

1. Outline of Thesis

These measurements were prompted by Miiller's work (1968,1969) on Palladium. In the $[0\zeta\zeta]T_1$ branch of the dispersion curves he found an anomalous increase of slope which could not be satisfactorily explained. This effect had not been observed in Nickel (Birgeneau et al.,1964) nor in Copper (Svensson et al.,1965) which are, like Palladium, face centred cubic metals.

Platinum is also an f.c.c. metal. It lies in the same group of the periodic table as Palladium and Nickel. Nickel is ferromagnetic at room temperature , Palladium is nearly so, Platinum is not. The study of Platinum could very well shed more light on the Palladium anomaly. Even were there no anomaly the force system of Platinum is of interest in its own right. Experiments on Platinum have already been performed by Orlich and Drexel (1968). However, their results are incomplete and not very precise since they were obtained by time of flight methods. The dispersion curves can be measured more precisely with a crystal spectrometer. For these reasons a study of the lattice dynamics of Platinum was undertaken. In Section 2 of this chapter we discuss briefly the history of such measurements. Sections 3 and 4 are devoted to explanations of the Born-von Kármán theory of Lattice Dynamics and the theory of neutron scattering.

Chapter 2 contains an analysis of the results in Platinum at 90°K. The force constants of the Born-von Kármán models are fitted to the measured dispersion curves. From the most realistic model a frequency distribution is calculated and used to evaluate C_v (specific heat) as a function of temperature.

In Chapter 3 the anomalous behaviour of Palladium and Platinum is considered in detail. Measurements of the $[0\zeta\zeta]T_1$ branch in Platinum at temperatures of 90, 296 and 473°K are reported. Off-symmetry measurements have been made in the (100) plane of Palladium in an attempt to determine the extent of the anomaly. An explanation of the anomaly as a Kohn Effect is advanced.

2. Lattice Dynamics: An Historical Sketch

The study of Lattice Dynamics is an attempt to correlate the motions of the atoms in a solid with the macroscopic thermodynamic properties of the solid. In the early part of this century there was no experimental information about these atomic motions. In lieu of this various models were put forward to explain the observed values of specific heats (C_v).

Einstein (1907) proposed that all the atoms in a solid be treated as simple harmonic oscillators. All these oscillators were to have the same frequency. The number of oscillators was chosen to give the correct number of degrees of freedom. This procedure gave values of C_v which tended to the correct high temperature limit but gave only qualitative

agreement at low temperatures, the values of C_v descending too rapidly with temperature.

The Einstein frequency distribution was just a delta function about some one frequency. The obvious next step was to propose a more complicated distribution. In 1912 two new models were put forward. Debye suggested that the frequency of the atomic oscillations should be a linear function of the wave vector. This amounted to considering a solid as an isotropic elastic continuum, which is a sound approach in the region where wavelengths are much greater than interatomic spacings. As we shall shortly see the extension to shorter wavelengths is not valid, but at any rate the frequency distribution arising from this hypothesis is proportional to the square of the frequencies. A maximum 'cut-off' frequency is chosen by normalizing the number of frequencies to the number of degrees of freedom. Values of C_v calculated in this approximation agreed well with the experimental values at high and low(where $C_v \propto T^3$)temperatures for most materials though metals required a correction for the electronic specific heat contribution (**Sommerfeld** , 1928). In the intermediate temperature region, however, the agreement was not satisfactory. This was because the real frequency distribution was more complicated yet.

The other model proposed in 1912 was that of Born and von Kármán. Where Einstein had suggested a set of uncoupled harmonic oscillators they, to use Born's own words, "remarked at once that Einstein's monochromatic formula ought to be

improved by taking the coupling of the vibrations into account". This procedure gives rise to dispersion in the frequency-wave vector relations. Since these relations had not been measured there was no way of deciding whether this approach was more correct than Debye's. Because of this and because the Debye model was simple and gave good qualitative results the ideas of Born and von Kármán lay dormant until the 1940's when measurement of the dispersion relations became possible.

The two most useful probes for measuring the oscillatory properties of solids are neutrons and X-rays. Of these two, neutrons are far and away the superior tool. The reasons for this are simple. Both X-rays and neutrons have wavelengths of the order of interatomic spacings. At these wavelengths the energies of X-rays are $\sim$5000 e.v. while those of neutrons are only of the order of tenths of an electron volt. This last is the same order of magnitude as the oscillatory energies of atoms in a solid. Thus while both X-rays and neutrons are ideal for measuring static properties of solids, where only momentum transfer is involved, only neutrons can provide the energy resolution necessary for accurate measurement of dynamic properties.

Notwithstanding this the first measurements of dispersion curves were made with X-rays since they were available before the advent of high flux reactors provided neutrons in sufficient quantities. It was suggested by Laval (1941) that the dispersion relations could be inferred from the intensities of thermal diffuse scattering of X-rays. The first measure-

ments were made by Olmer (1948) in the (100) direction of Aluminium. Work on β-Brass (Cole and Warren, 1952), Iron (Curien, 1952), Copper (Jacobsen, 1955) and Aluminium (Walker, 1956) followed. In all these measurements corrections for many different factors had to be made to the measured intensities. Bearing in mind that absolute intensities are difficult things to measure in the first place, it is not surprising that most of these measurements were quantitatively incorrect. However they did indicate the dispersion that Born and von Kármán had predicted.

In 1954 Placzek and Van Hove suggested that the dispersion relations could be measured by the inelastic scattering of thermal neutrons. Others had had the same idea and experimental work was already under way when this paper appeared. Aluminium was the first material to be studied in this fashion by Brockhouse and Stewart (1955,1958) and Carter, Hughes and Palevsky (1957). These initial results were not very accurate but by 1958 Brockhouse and Iyengar had made measurements in Germanium with an accuracy of 4-5%. The real flowering of the subject awaited the development of the Triple Axis Crystal Spectrometer and the subsequent ability to make measurements with constant momentum or constant energy transfer (Brockhouse, 1961). Since that time results have been obtained for many materials and the theory of Born and von Kármán has been used extensively in analyzing these measurements. At the same time other force models have been proposed since the Born-von Kármán model is unsatisfactory on at least two

counts. First the atomic motions are not strictly harmonic and second the model yields only the magnitudes of the forces between the atoms. It tells nothing of the sorts and conditions of the forces. For the purposes of this thesis these drawbacks are not serious. The model will be quite sufficient for our present needs. In the next few pages we will describe the lattice dynamics of Platinum in terms of this model.

3. The Born-von Kármán Theory of Lattice Dynamics

Platinum is a face centred cubic metal having one atom per unit cell. The equilibrium positions of the atoms are the lattice points given by

$$\vec{r}(\ell) = \ell_1(\vec{a}_1) + \ell_2(\vec{a}_2) + \ell_3(\vec{a}_3) \qquad \text{I-1}$$

where ℓ_1, ℓ_2 and ℓ_3 are integers and $\vec{a}_1$, $\vec{a}_2$ and $\vec{a}_3$ are the basis vectors of the lattice (in this case they are $(\frac{1}{2},\frac{1}{2},0)$, $(\frac{1}{2},0,\frac{1}{2})$, $(0,\frac{1}{2},\frac{1}{2})$. These atoms are continuously oscillating about their equilibrium positions. We want to calculate the dynamics of these oscillations using the theory of Born and von Kármán (1912). To do this we must make some approximations.

First we must assume that each atom can be treated as an integral unit. That is, we do not have to worry about the separation of nucleus and electrons. We say that the electrons move so much faster then the nucleus that they follow its motion adiabatically (hence the name 'Adiabatic Approximation'). That such an approximation is valid in a metal where some of the electrons are known to be free is a moot point. However Ziman (1964) and Cochran (1965) have shown that an ion and its electronic screening charge can be treated

as a neutral 'pseudo-atom' which, with a suitably defined crystal potential, will lend itself to calculations of this sort.

The other assumption we must make is called the Harmonic Approximation. We propose that each atom makes only small oscillations about its equilibrium position, which enables us to treat each atom as an harmonic oscillator. The potential energy (ϕ) of the lattice will consist of a static equilibrium term (ϕ_o) and a part that depends on the oscillations of the atoms. Suppose the displacement of the ℓ^{th} atom from its equilibrium position is $\vec{u}(\ell)$. We may expand the potential energy as a Taylor's series in these displacements.

$$\phi = \phi_o + \sum_{\ell,\alpha} \left(\frac{\partial \phi}{\partial u_\alpha(\ell)}\right)_o u_\alpha(\ell) + \frac{1}{2} \sum_{\substack{\ell,\alpha \\ \ell',\beta}} \left(\frac{\partial^2 \phi}{\partial u_\alpha(\ell)\, \partial u_\beta(\ell')}\right)_o u_\alpha(\ell) u_\beta(\ell') \quad \text{I-2}$$

$$+ \text{ higher order terms}$$

where α, β are Cartesian co-ordinates and the sums are carried out over all co-ordinates of all atoms. The partial derivatives in this expression are evaluated at the equilibrium positions of the atoms.

The Harmonic Approximation consists of ignoring all terms of higher than second order in $\vec{u}(\ell)$. This restriction does not allow us to calculate such properties as thermal expansion or phonon lifetimes. Such anharmonic properties may be calculated by introducing the higher order terms as a perturbation of the harmonic situation. These 'quasi-harmonic' calculations will not be discussed here. The Harmonic Approximation will suffice for our purposes.

We can simplify the expression for ϕ in a number of ways.

First we note that $\frac{\partial \phi}{\partial u_\alpha(\ell)}$ is the net force on the ℓ^{th} atom in the α^{th} direction. In equilibrium this force must be zero. Therefore the second term in Eq. 1-2 vanishes. If we now simplify the notation by putting

$$\left(\frac{\partial^2 \phi}{\partial u_\alpha(\ell)\partial u_\beta(\ell')}\right)_0 = \phi_{\alpha\beta}(\ell,\ell') \qquad \text{I-3}$$

then Eq. 1-2 becomes

$$\phi = \phi_o + \frac{1}{2}\sum_{\substack{\ell,\alpha \\ \ell',\beta}} \phi_{\alpha\beta}(\ell,\ell')u_\alpha(\ell)u_\beta(\ell') \qquad \text{I-4}$$

In order to set up the equations of motion of the lattice we must also know the kinetic energy of the atoms. This may be written as

$$T = \frac{1}{2} M \sum_{\ell,\alpha} [\dot{u}_\alpha(\ell)]^2 \qquad \text{I-5}$$

where M is the mass of the Platinum atom. So the Hamiltonian of our system becomes

$$\begin{aligned} \mathcal{H} &= T + \phi \\ &= \frac{1}{2} M \sum_{\ell,\alpha} [\dot{u}_\alpha(\ell)]^2 + \phi_o + \frac{1}{2}\sum_{\substack{\ell,\alpha \\ \ell',\beta}} \phi_{\alpha\beta}(\ell,\ell')u_\alpha(\ell)u_\beta(\ell') \end{aligned} \qquad \text{I-6}$$

Using Hamilton's equations we can work out the equation of motion of the ℓ^{th} atom. This equation is

$$M\,\ddot{u}_\alpha(\ell) = -\sum_{\ell'\beta} \phi_{\alpha\beta}(\ell,\ell')u_\beta(\ell') \qquad \text{I-7}$$

The term on the right hand side of Eq. 1-7 is the net force exerted on the atom at ℓ in the α^{th} direction. The $\phi_{\alpha\beta}(\ell,\ell')$ can therefore be interpreted as force constants. That is they represent the force in the direction α on the ℓ^{th} atom when the atom at ℓ' is displaced a unit distance in the direction β. From the translational symmetry of the lattice such a force constant can depend only on the separation, $\vec{r}_\ell - \vec{r}_{\ell'}$, of the atoms at ℓ and ℓ'. Further there is no reason why we should not translate the origin to the

lattice site ℓ. Then the equation becomes

$$M\,\ddot{u}_\alpha(0) = -\sum_{\ell'\beta} \phi_{\alpha\beta}(\ell')u_\beta(\ell') \qquad \text{I-8}$$

The equation we want to solve is now set up. We would like eventually to determine the atomic force constants since they can tell us something of the nature of the forces between the atoms. Let us now consider a travelling wave solution of the form

$$u_\alpha(\ell) = \frac{1}{\sqrt{M}}\, u_\alpha\, e^{-i[\omega t - \vec{q}\cdot\vec{r}(\ell)]} \qquad \text{I-9}$$

where u_α = a constant times a unit polarization vector $(\vec{\xi}_\alpha(\vec{q},j))$.

ω = the angular frequency of the wave

and $\vec{q}$ = the wave vector

substituting this into Eq. 1-8 we obtain

$$\omega^2 u_\alpha = \frac{1}{M} \sum_{\ell'\beta} \phi_{\alpha\beta}(\ell')u_\beta\; e^{i\vec{q}\cdot\vec{r}(\ell')} \qquad \text{I-10}$$

Define

$$D_{\alpha\beta}(\vec{q}) = \frac{1}{M} \sum_{\ell'} \phi_{\alpha\beta}(\ell')\; e^{i\vec{q}\cdot\vec{r}(\ell')} \qquad \text{I-11}$$

Then Eq. 1-10 becomes

$$\omega^2 u_\alpha = \sum_\beta D_{\alpha\beta}(\vec{q})u_\beta \qquad \text{I-12}$$

The $D_{\alpha\beta}(\vec{q})$ are the elements of the so called Dynamical Matrix. For each value of $\vec{q}$ there will be three equations, one for each Cartesian co-ordinate. These three equations will have a solution if and only if

$$\det.|D_{\alpha\beta} - \omega^2\delta_{\alpha\beta}| = 0 \qquad \text{I-13}$$

Hence for each value of $\vec{q}$ there will be three frequencies,

i.e. three modes of oscillation. It now remains to determine how many values of $\vec{q}$ there are.

This we do by imposing boundary conditions on the crystal. We shall use the 'cyclic' boundary conditions of Born and von Kármán, to wit:

$$u(\ell+L) = u(\ell) \qquad \text{I-14}$$

where $$\vec{r}(L) = L_1(\vec{a}_1) + L_2(\vec{a}_2) + L_3(\vec{a}_3) \qquad \text{I-15}$$
$$= \text{some lattice vector.}$$

The product $N = L_1L_2L_3$ gives the number of unit cells in the volume over which we insist the wave function must repeat. Now we know from the Bloch theorem that a wave in a crystal lattice can only differ by a phase factor from lattice point to lattice point, i.e.

$$u(\ell+L) = e^{i\vec{q}\cdot\vec{r}(L)}u(\ell) \qquad \text{I-16}$$

Therefore from our boundary condition 1-14 we see that

$$e^{i\vec{q}\cdot\vec{r}(L)} = 1$$

Hence considering translations in the direction of the three unit vectors we see that

$$e^{i\vec{q}\cdot L_1\vec{a}_1} = e^{i\vec{q}\cdot L_2\vec{a}_2} = e^{i\vec{q}\cdot L_3\vec{a}_3} = 1 \qquad \text{I-17}$$

Then $\vec{q}$ may be written as

$$\vec{q} = 2\pi\left(\frac{h_1}{L_1}\vec{b}_1 + \frac{h_2}{L_2}\vec{b}_2 + \frac{h_3}{L_3}\vec{b}_3\right) \qquad \text{I-18}$$

where h_1, h_2 and h_3 are integers and $\vec{b}_1, \vec{b}_2$ and $\vec{b}_3$ are basis vectors of the reciprocal lattice with the property that

$$\vec{a}_i\cdot\vec{b}_j = \delta_{ij} \qquad \text{I-19}$$

An inspection of the expression for $u_\alpha(\ell)$ will show that we can restrict the values of $\vec{q}$ to those provided by

the following range of integers:

$$h_1 \equiv -L_1/2 \text{ to } L_1/2$$
$$h_2 \equiv -L_2/2 \text{ to } L_2/2$$
$$h_3 \equiv -L_3/2 \text{ to } L_3/2$$

This range of $\vec{q}$ defines the first Brillouin zone. (Cross sections of the 100 and $1\bar{1}0$ planes in the reciprocal lattice of a face centred cubic lattice are shown in Fig. I-1. The boundaries of the first Brillouin zones in these planes are outlined). Any other values of $\vec{q}$ can be related to values within this zone by the addition of a suitable reciprocal lattice vector. All the possible values of $\vec{q}$ are therefore covered by the values of $\vec{q}$ within this zone. We see that there are $N(=L_1L_2L_3)$ such values. Since there exist three frequencies for each value of $\vec{q}$ we may conclude that our crystal has 3N possible modes of vibration.

It would seem then that assiduous measurement of the values of ω for various wave vectors will allow us to calculate the interatomic force constants. We will shortly show that it is possible to measure the frequency-wave vector relations. Is it now possible to invert this data to yield the force constants? Unless we also know the polarization vectors ($\vec{\xi}$) corresponding to each ω it is not. In general the polarization vectors are difficult to assign. If however the wave vector $\vec{q}$ points in a major symmetry direction the Dynamical Matrix factorizes and the polarization vectors are fixed by the symmetry of the lattice. The waves in this case can only be transverse or longitudinal which as we shall see

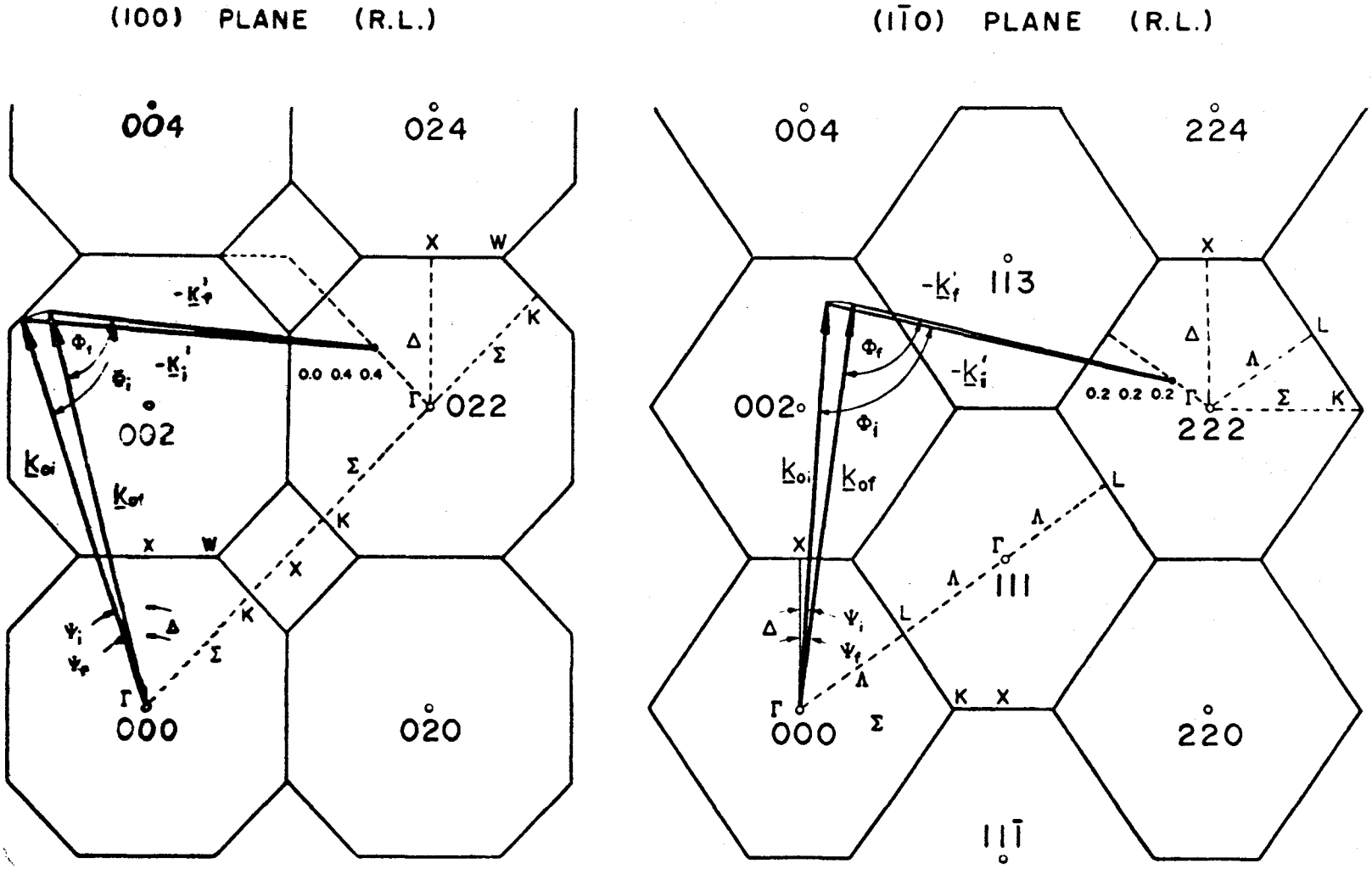

Figure I-1: The (100) and (1$\bar{1}$0) planes of the reciprocal lattice of an f.c.c. lattice showing the boundaries of the first Brillouin zones. The vectors 'k' represent the initial and final neutron wave vectors for Constant-$\vec{Q}$ scans of two transverse modes, one at wave vector $\vec{q}$ = (0,0.4,0.4)$2\pi/a$ and one at $\vec{q}$ = (0.2,0.2,0.2)$2\pi/a$

greatly simplifies the measurements. Also the expression for ω^2 becomes linear in the force constants. It may be written

$$M\omega^2 = \sum_n \phi_n(1-\cos(n\pi q/q_m)) \qquad \text{I-20}$$

for a particular branch in a given symmetry direction. Here q_m is one half the distance from the origin to the nearest reciprocal lattice point in the specified symmetry direction and ϕ_n is a linear combination of interatomic force constants $\phi_{\alpha\beta}$ for which $\vec{q}\cdot\vec{r}(\ell')$ is a constant (see Eq. 1-10). Since $\vec{q}\cdot\vec{r}(\ell')$= a constant defines a plane perpendicular to $\vec{q}$ the ϕ_n are called interplanar force constants. (Foreman and Lomer 1957).

Now we have sufficient information to invert these ω^2-q relations and obtain values for the ϕ_n. Given enough linear combinations ϕ_n we may solve for the $\phi_{\alpha\beta}$'s. In a face centred cubic crystal this may be done provided we consider only interactions out to fourth nearest neighbours. If we try to solve for more neighbours we get more unknown $\phi_{\alpha\beta}$'s than equations. In this case we may use the symmetry of the crystal to apply additional constraints to the force constants. The constraint equations necessary to solve six and eight neighbour models are given in Table II-3.

To sum up then, the Born-von Kármán theory predicts that there will be dispersion in the frequency-wave vector relations. If these relations can be measured in the major symmetry directions then we can Fourier analyze the curves to determine the interatomic force constants. Let us now see

how we can use neutrons to make these measurements.

4. Scattering of Neutrons from Single Crystals

We want to consider the scattering of neutrons from a system of N atoms. We will assume some interaction potential V(r) which depends only on the separation of neutron and nucleus. In the first Born approximation (Schiff,1968) the differential scattering cross section per unit energy per unit solid angle is (Van Hove 1954)

$$\frac{\partial^2\sigma}{\partial\Omega\partial\varepsilon} = A\, S(\vec{Q},\omega) \qquad \text{I-21}$$

Where

$$A = \frac{m^2}{4\pi^2\hbar^5}\frac{k'}{k_o}\left[\int \exp(i\vec{Q}\cdot\vec{r})V(r)\,dr\right]^2$$

and

$$S(\vec{Q},\omega) = \sum_n g(n)\left|< m\right| \sum_{j=1}^{N} \exp(i\vec{Q}\cdot\vec{r}_j)\left|n>\right|^2 \delta(E'-E_o-\hbar\omega)$$

and m = the mass of the neutron

$\vec{Q}$ = the momentum transfer to the system

$\hbar\omega$ = the energy transfer to the system

E_o, E' = the incident and scattered neutron energies

k_o, k' = the incident and scattered wave vectors

$|m>, |n>$ = the initial and final states of the scattering system

$g(n)$ = a statistical population factor for the state $|n>$

This cross section may be split into a coherent and an incoherent part (Placzek and Van Hove, 1954), the first arising from the ordered motions of the atoms, the second from the variation of the scattering length from atom to atom. We are interested in the coherent part, in particular the one phonon

coherent cross section. We may ignore the incoherent scattering since, in our measurements, it gives rise only to a continuous background with no distinctive features. This is tantamount to assuming the scattering length to be the same for all atoms in the system.

Now we must define the interaction potential V(r). We do not know its actual form but the so called 'Fermi pseudopotential' (Fermi,1936) serves the purpose.

$$V(r) = \left(\frac{2\pi a\hbar^2}{m}\right)\delta(r) \qquad \text{I-22}$$

where a = scattering length of the system's nuclei.

Then Eq. 1-21 becomes

$$\frac{\partial^2\sigma}{\partial\Omega\partial\varepsilon} = a^2/\hbar\ k'/k_o\ S(\vec{Q},\omega) \qquad \text{I-23}$$

Evidently then if we wish to determine the scattering cross section the variables to measure are energy and momentum transfer to and from the system.

If we now insert the values of $\vec{r}_j$ (which we know from the discussion of the previous section) in $S(\vec{Q},\omega)$ and perform the necessary manipulations we end up with a series of terms describing the various processes that can occur within the scattering system. The cross section for one such process, the creation (or annihilation) of a single phonon is

$$\frac{\partial^2\sigma}{\partial\Omega\partial\varepsilon} = (2\pi)^3\ \hbar N/V\ a^2\ \frac{k'}{k_o}\ \exp\ [-2W(\vec{Q})]\ \begin{pmatrix} N_j(\vec{q}) \\ N_j(\vec{q})+1 \end{pmatrix}$$

$$\times\ \frac{[\vec{Q}\cdot\vec{\xi}(\vec{q},j)]^2}{2m\omega_j(\vec{q})}\ \delta(\vec{Q}-2\pi\vec{\tau}-\vec{q})\,\delta(E_o-E'-\hbar\omega) \qquad \text{I-24}$$

where N = the number of atoms in the volume V

$W(\vec{Q}) = \frac{1}{2}\langle[\vec{Q}\cdot\vec{u}(\ell)]^2\rangle$

and $\exp(-2W(\vec{Q}))$ = the Debye-Waller factor

$N_j(\vec{q}) = [\exp(\hbar\omega_j(\vec{q})/kT)-1]^{-1}$

= the Bose-Einstein population factor for phonon annihilation processes

$N_j(\vec{q})+1$ = the population factor for phonon creation processes

$\vec{\tau}$ = a reciprocal lattice vector

$\vec{\xi}(\vec{q},j)$ = the polarization vector of the phonon

Phonon creation processes are those in which the incident neutrons lose energy upon scattering; phonon annihilation processes, those in which the incident neutrons gain energy.

There are other processes which may occur within the scattering system. For instance, the neutrons might be scattered elastically. In this case the conditions on the energy and momentum are

$$E_o = E'$$
$$\vec{Q} = 2\pi\vec{\tau} \qquad \text{for some } \vec{\tau} \qquad \text{I-25}$$

In general this Bragg scattering yields very sharp and intense peaks in the scattered neutron distribution. It will not be too difficult to separate such peaks from the one phonon neutron groups. There are also processes in which more than one phonon is created (or destroyed). Then the dynamical conditions are

$$E'-E_o = \hbar\omega_1+\hbar\omega_2+.....$$
$$\vec{Q} = 2\pi\vec{\tau}+\vec{q}_1+\vec{q}_2+..... \qquad \text{I-26}$$

Such processes will give no sharp peaks in the scattered distribution. The scattering will contribute to the background of course but it will be a continuous contribution. Under these circumstances it should be relatively easy to separate the groups of neutrons scattered by one phonon processes from the rest of the scattered neutrons.

Let us now consider the one phonon cross section (Eq. 1-24) in some detail. First we see that neutrons which create or annihilate a phonon will be scattered in groups having well defined values of energy and momentum

$$E_o - E' = h\omega$$
$$\vec{k}_o - \vec{k}' = \vec{Q} = 2\pi\vec{\tau} + \vec{q} \qquad \text{I-27}$$

Each pair $(\omega,\vec{q})$ will belong to one of the branches (j) of the dispersion curves and will give one point on that branch. We want to know what factors in Eq. 1-24 can be arranged to optimize the intensity of the neutron group for a given phonon. $(\omega,\vec{q})$.

Consider the term $(\vec{Q}\cdot\vec{\xi})^2$. It will be to our advantage to make $\vec{Q}$ as nearly parallel as possible to the $\vec{\xi}$ we want. We have already mentioned (see Sec. 1-3) that in a direction of major symmetry the waves must be either wholly transverse or wholly longitudinal (i.e. $\vec{\xi}$ must be either perpendicular or parallel to $\vec{q}$). If then $\vec{Q}$ is nearly parallel to the desired $\vec{\xi}$ it will be nearly perpendicular to the two other polarization vectors. That is $(\vec{Q}\cdot\vec{\xi})^2$ will be a maximum for one $\vec{\xi}$ and nearly zero for the other two since the three polarization vectors are mutually perpendicular.

In addition to fixing the direction of $\vec{Q}$ we would do well to make $|\vec{Q}|$ as large as possible. Here the restriction is that if $\vec{Q}$ gets too large the Debye-Waller factor ($\exp(-2W(\vec{Q}))$ becomes small. However $|\vec{Q}|$ is likely to be limited by the values of $|\vec{k}_o|$ and $|\vec{k}'|$ before this factor becomes important.

The temperature of the sample can also affect the measurements. At low temperatures ($\sim$1°K) the population factor N_j becomes very small making phonon creation processes the only practicable measurements. At temperatures near the melting point the amplitudes of oscillation become large and the Debye-Waller factor gets small. Neither of these considerations affect the present measurements very strongly since the work was done between 90 and 473°K.

The direction and magnitude of $\vec{Q}$ then seem to be the principal factors controlling the intensity. We want to be able to pre-select both these quantities. As well, we want the capability of holding $\vec{Q}$(i.e.$\vec{q}$) constant while scanning through the range of ω (or vice versa). All these conditions can be met with a Triple Axis Crystal Spectrometer (Brockhouse, 1961) which we shall investigate in the next chapter.

CHAPTER II

THE LATTICE DYNAMICS OF PLATINUM

1. Introduction

We mentioned in Section I-1 that the primary reason for studying Platinum was to see if it would display anomalous behaviour similar to that observed in Palladium. We will be discussing this aspect of the problem in Chapter III where a possible explanation of the effect in both metals is advanced. In this chapter the anomaly is ignored while the general force system of Platinum is elucidated using a Born-von Kármán model. From the most realistic model a frequency distribution is calculated and used to evaluate C_v as a function of temperature.

The measurement of the dispersion curves was made at 90°K. This temperature was chosen, rather then room temperature, in order that any anomalous behaviour might be enhanced (see Chapter III). All this work was done on the McMaster University Triple Axis Spectrometer at Chalk River. Before we plunge into a detailed discussion of the measurements a description of this instrument is in order.

2. Triple Axis Spectrometer

We have seen that in order to measure one phonon processes we must be able to observe various energy transfers and various momentum transfers. In addition we want to be able to hold one of these quantities constant while scanning the range

of the other. Therefore we want to be able to control the incident and scattered energies (E_o and E') and the incident and scattered momenta ($\vec{k}_o$ and $\vec{k}'$) both in magnitude and direction. We can do all this with a Triple Axis Spectrometer. This instrument has been discussed in detail by various authors, (Brockhouse ,1961; Brockhouse et al.,1964; Iyengar,1965; Rowe,1966; Brockhouse et al.,1968). A schematic diagram of the apparatus used in these measurements is given in Fig. II-1. With the aid of this diagram let us briefly consider the operation of such a spectrometer.

A beam of white neutrons emerging from a reactor is monochromated by Bragg reflection from the (220) planes of a Copper crystal. In our case a double reflection monochromator (Brockhouse, deWit, Hallman and Rowe, 1968) is used. Since the monochromated beam always emerges parallel to the incident beam the monochromator may be inserted directly in the beam tube behind the reactor face. This obviates the need for cumbersome movable shielding which always accompanies a single crystal monochromator. Rotating the monochromator gives a continuous range of values of E_o (and hence $|\vec{k}_o|$). The monochromatic beam is allowed to fall on the sample (S) after passing through a suitable collimator (C_2). A good deal of collimation is provided simply by the length of the beam tube (C_o and C_1) and C_2 can be varied to suit the needs of an individual experiment.

The direction of $\vec{k}_o$ is fixed relative to the reciprocal space of the sample by rotating the sample (angle ψ in Fig. II-1).

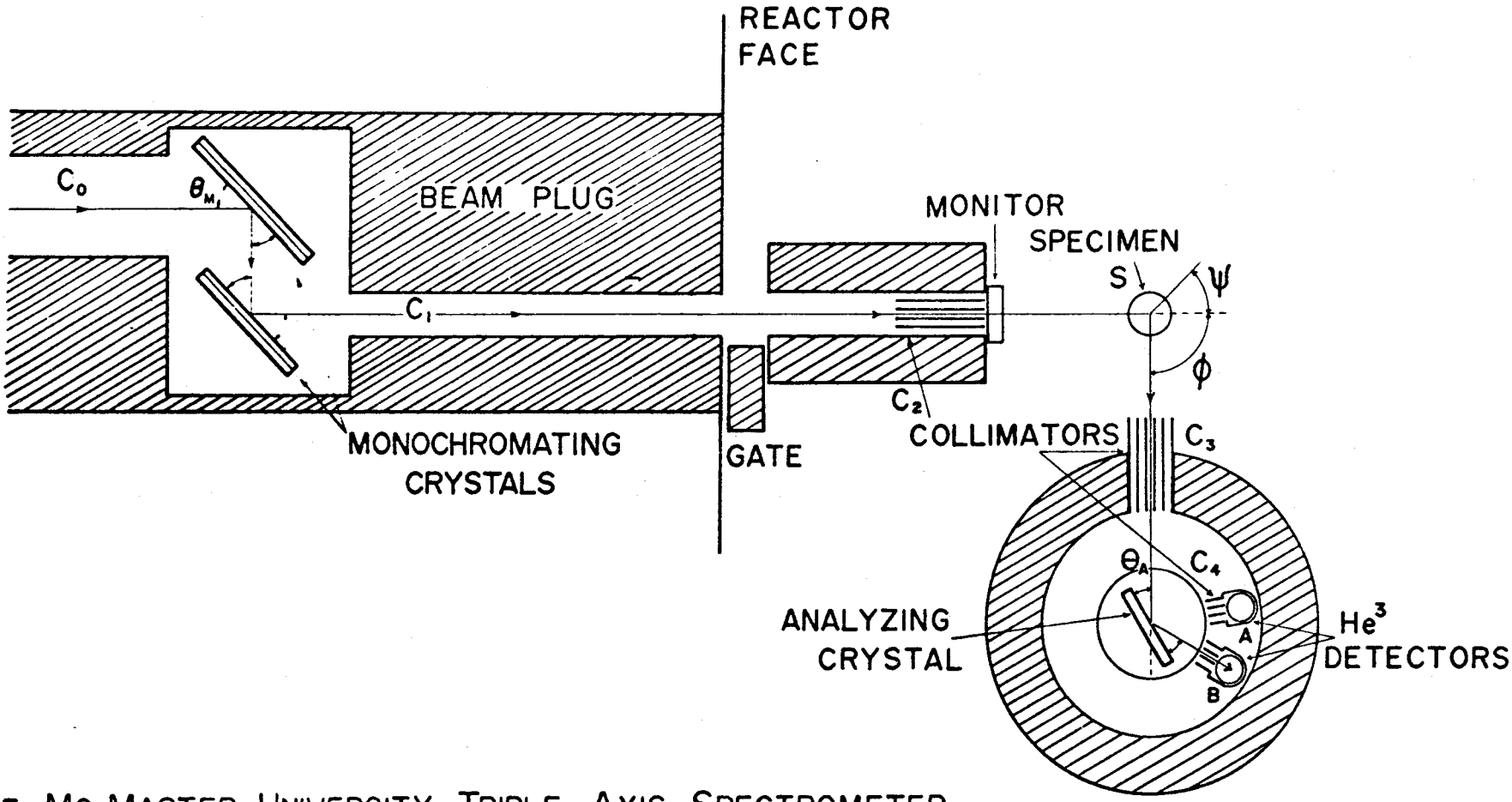

THE MC MASTER UNIVERSITY TRIPLE AXIS SPECTROMETER
AT CHALK RIVER (E 2 BEAM PORT)
SCHEMATIC DIAGRAM, NOT TO SCALE

FIGURE II-1

The direction of $\vec{k}'$ is fixed by setting the analyzing unit to some angle ϕ with respect to the direction of the incident beam. E' and hence the magnitude of $\vec{k}'$ are set by Bragg reflection from another Copper crystal (this time from the (200) planes). Again the rotation of this crystal provides a continuous range of values for E'. The neutrons scattered by this final reflection are detected by a He_3 counter (B). The second detector (A) records background radiation in the the analyzer unit. Soller slit collimators are placed between the sample and the analyzing crystal (C_3) and between the crystal and the counter (C_4). The latter provides only very coarse collimation.

The most convenient way to use this spectrometer is in the 'Constant-Q' mode (Brockhouse,1961). We said earlier that one of $\vec{q}$ or ω needs to be held constant while the other is varied. Suppose we fix the momentum transfer $\vec{Q} = \vec{k}' - \vec{k}_o$. Let us also fix the incident energy E_o. If we vary E' by rotating the analyzing crystal we will also vary $\vec{k}'$ (since $E = \frac{\hbar^2 k^2}{2m}$). Therefore the only way to keep $\vec{Q}$ constant is to vary the direction of $\vec{k}_o$ and $\vec{k}'$ in concert with the variation in E'. With the triple axis spectrometer this is done by changing ψ and ϕ (i.e. by changing the orientation of $\vec{k}_o$ with respect to the reciprocal space of the sample and by changing the scattering angle. The beginning and end points of two 'Constant-Q' phonons are shown in Fig. I-1.

Alternatively we might have held E' constant and varied E_o. In some circumstances this is the better of the two methods.

Again, with this instrument it is equally possible to keep the energy transfer constant while scanning through $\vec{Q}$(i.e.$\vec{q}$). This 'Constant-E' method provides better resolution than 'Constant-Q' where the slope of the dispersion curve is very steep (as for instance near the origin of $\vec{q}$). All these various methods have been discussed in detail by Brockhouse et al. (1961). We shall not linger upon them here. Nor will we go into the details of the spectrometer operation. There are various aspects, such as focussing, which are functions of the types and arrangements of monochromators and collimation. These things are peculiar to each spectrometer.

3. Experimental Results

All the present measurements were made on the spectrometer described above. The Constant-Q mode was used throughout the work.

The single crystal of Platinum used as a sample was a cylindrical boule with a [100] axis at an angle of about 20° to the cylinder's axis. It was grown by Materials Research Corporation and was about 2" long by 1/4" in diameter. It had a mosaic spread of about 12' as measured by rocking the crystal against a reflection from the (311) plane of a perfect Germanium crystal. The stated purity of the material used was 99.99%.

Various incident energies were used in the course of the measurements. Table II-1 gives the incident energies in units of frequency, wavelength, and energy. It also gives the

angles of reflection from the (220) plane of the Copper monochromator. The rest of this discussion will be carried on in frequency units.

Table II-1

The various incident energies used in the experiment are given here, in units of energy, frequency and wavelength. $2\theta_M$ is the angle of scattering from the (220) plane of the Copper monochromator.

$2\theta_M$ (Degrees)	E (m.e.v.)	ν (10^{12}cps)	λ (A°)
82.18	29.00	7.0157	1.6798
70.76	37.35	9.0299	1.4800
63.12	45.70	11.0498	1.3379
55.54	57.70	13.9513	1.1907

The lower transverse branches were studied thoroughly at high resolution in an attempt to ferret out any anomalous behaviour. The incident frequency here was 7.02×10^{12} cps. Some of the lowest frequencies were measured with vertical collimation of the order of 0.6° as well as horizontal collimation of the same order in the incident beam. Most of the measurements were made with horizontal collimation only, in both the incident and scattered beams.

The other branches of the dispersion curves were measured with higher incident frequencies. In order to get decent intensities for the neutron groups at the zone

boundaries in the longitudinal branches it was necessary to use an incident frequency of 13.9 x 10^{12} cps (with consequent loss of resolution). This state of affairs was not unexpected since the crystal was not overly large and intensities are not very high at 90°K anyway. In most cases it was possible to obtain reasonably well formed neutron groups. Fig. II-2 shows a representative sample of these groups, one from each branch.

The resultant dispersion curves are shown in Fig. II-3, where frequency is plotted against reduced wave vector for the four major symmetry directions. The symmetry points and directions are labelled after the style of Bouckaert et al. (1936). A list of frequencies is given in Table II-2. The $[0\zeta\zeta]T_1$ branch is listed separately in Table III-1. The velocities of sound have been calculated from the elastic constants of Macfarlane and Rayne (1965) and compared to the initial slopes of the dispersion curves. The slopes of the solid straight lines in Fig. II-3 represent these sound velocities. The agreement can be seen to be quite satisfactory.

We note in passing the obvious kink in the $[0\zeta\zeta]T_1$ branch. The curve has a point of minimum slope at reduced wave vector $\zeta \simeq 0.33$ and frequency ~ 1.5 x 10^{12} cps. Beyond this point the slope increases before decreasing to zero in the normal way. The effect is similar though not identical to that observed in Palladium. As we said this matter will be fully discussed in Chapter III. For now we will ignore it.

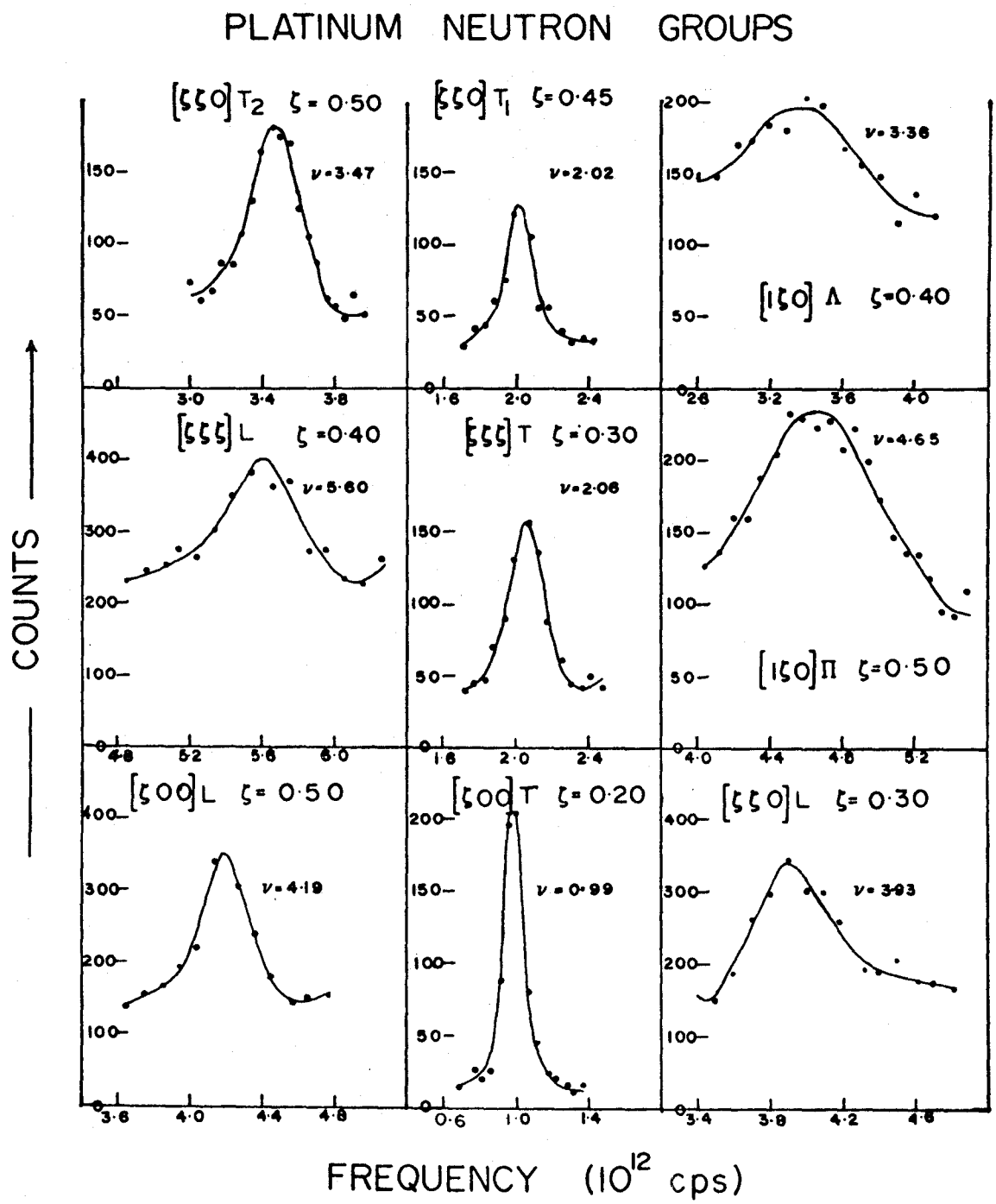

Figure II-2: Representative neutron groups from each of the branches of the dispersion curves of Platinum. The three groups in the centre column were measured at high resolution.

Table II-2: Normal mode frequencies (units of 10^{12}cps.) for Platinum at 90°K. The T_1 branch is listed in Table III-1.

BRANCH	ζ	FREQUENCY	BRANCH	ζ	FREQUENCY
$[00\zeta]T$	0.10	0.48 (0.02)	$[0\zeta\zeta]T_2$	0.10	0.70 (0.02)
	0.15	0.75 (0.02)		0.15	1.05 (0.02)
	0.20	1.01 (0.02)		0.20	1.38 (0.02)
	0.25	1.23 (0.02)		0.25	1.72 (0.02)
	0.30	1.48 (0.03)		0.30	2.03 (0.02)
	0.35	1.71 (0.02)		0.35	2.36 (0.04)
	0.40	1.98 (0.02)		0.40	2.53 (0.03)
	0.45	2.22 (0.02)		0.45	3.10 (0.03)
	0.50	2.45 (0.03)		0.50	3.47 (0.03)
	0.55	2.70 (0.02)		0.55	3.85 (0.02)
	0.60	2.93 (0.03)		0.60	4.21 (0.03)
	0.65	3.09 (0.03)		0.70	4.87 (0.03)
	0.70	3.30 (0.03)		0.80	5.36 (0.05)
	0.80	3.57 (0.04)		0.90	5.66 (0.07)
	0.90	3.76 (0,04)		1.00	5.84 (0.08)
	1.00	3.84 (0.05)			
			$[0\zeta\zeta]L$	0.10	1.49 (0.04)
$[00\zeta]L$	0.20	1.99 (0.05)		0.15	2.14 (0.03)
	0.30	2.79 (0.04)		0.20	2.82 (0.04)
	0.40	3.52 (0.05)		0.25	3.40 (0.05)
	0.50	4.19 (0.03)		0.30	3.94 (0.05)
	0.60	4.77 (0.03)		0.325	4.20 (0.08)
	0.70	5.18 (0.03)		0.40	4.77 (0.05)
	0.80	5.56 (0.04)		0.50	4.95 (0.06)
	0.90	5.73 (0.05)		0.60	4.93 (0.05)
	1.00	5.84 (0.08)		0.75	4.33 (0.07)
				0.90	3.89 (0.06)
$[\zeta\zeta\zeta]T$	0.10	0.76 (0.02)		1.00	3.84 (0.05)
	0.15	1.07 (0.02)			
	0.20	1.41 (0.03)	$[1\zeta 0]\lambda$	0.10	3.78 (0.08)
	0.25	1.74 (0.02)		0.30	3.49 (0.04)
	0.30	2.10 (0.02)		0.40	3.36 (0.05)
	0.40	2.63 (0.02)		0.50	3.28 (0.05)
	0.50	2.90 (0.02)			
			$[1\zeta 0]\pi$	0.10	5.73 (0.09)
$[\zeta\zeta\zeta]L$	0.10	1.76 (0.05)		0.20	5.58 (0.07)
	0.15	2.64 (0.03)		0.30	5.28 (0.07)
	0.20	3.44 (0.06)		0.40	4.95 (0.07)
	0.30	4.77 (0.04)		0.50	4.65 (0.07)
	0.40	5.60 (0.04)		0.60	4.44 (0.08)
	0.50	5.85 (0.05)		0.75	4.03 (0.05)

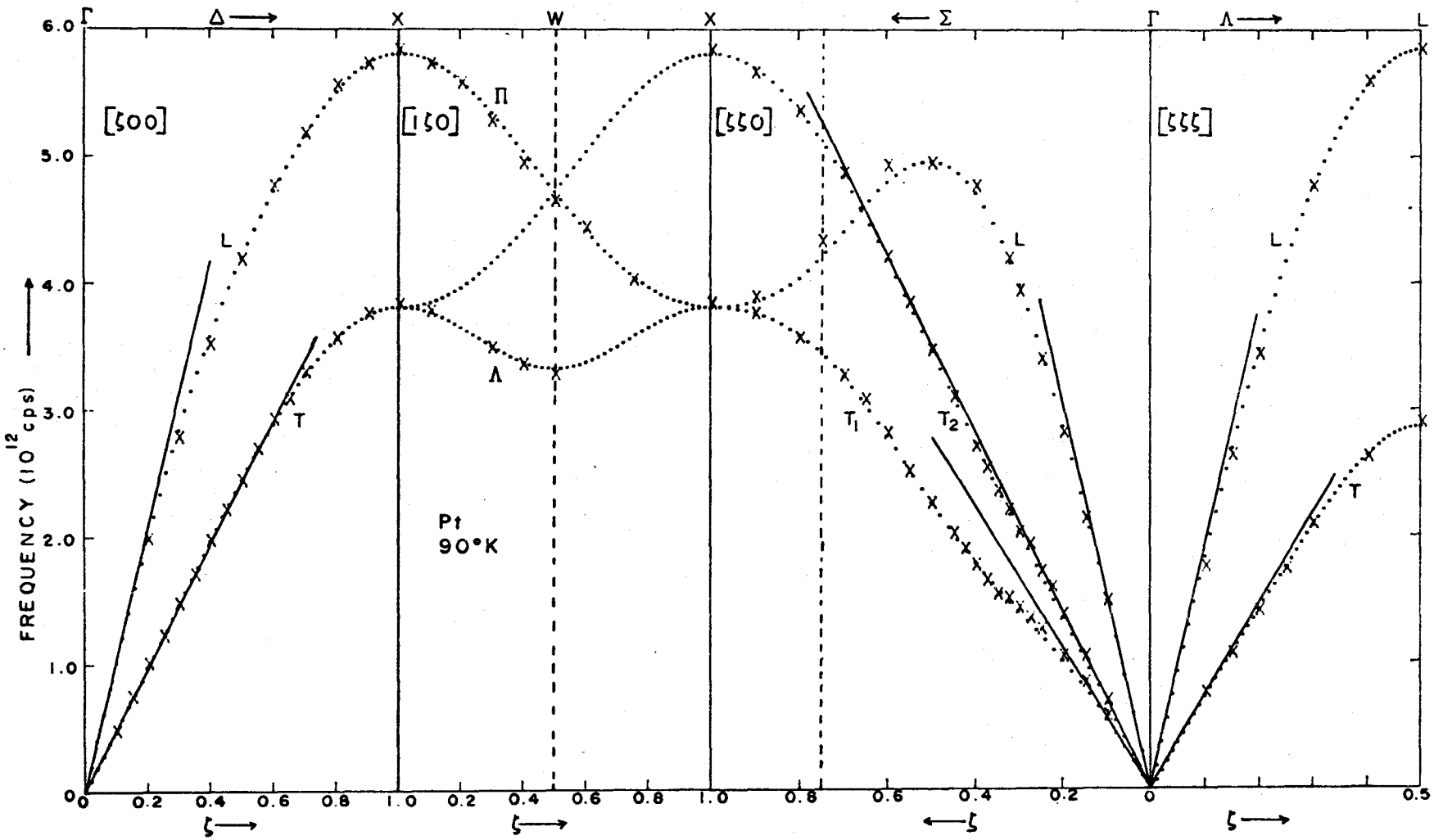

Figure II-3: The dispersion curves of Platinum at 90°K. The symbols 'x' represent the experimental points. The dotted line represents a sixth neighbour Born-von Kármán fit to the frequencies. The slopes of the solid straight lines are the velocities of sound in the various directions.

4. Discussion and Analysis of Results

With the exception of the $[0\zeta\zeta]T_1$ branch the dispersion curves of Fig. II-3 are what one would expect for a face centred cubic metal. They are in reasonable agreement with the time of flight measurements of Orlich and Drexel (1968) though these latter results are incomplete and do not show the anomaly in the T_1 branch.

The accuracy of the frequencies listed in Table II-2 is decided by considering the width, shape and counting statistics of the neutron groups (Brockhouse et al., 1962; Woods et al., 1962; Birgeneau et al., 1964). This method, which was generally used in earlier measurements of this type is now believed (Svensson et al., 1965) to yield errors which are of the order of two standard deviations. That is the errors listed in Table II-2 are probably too large. They may be considered as upper limits on the possible errors. Miiller (1969), after a careful analysis of the possible sources of error in a triple axis spectrometer puts the accuracy of the frequencies at about 0.7 to 0.8%. So the frequencies in Table II-2 are probably a little more accurate than is indicated.

Having the dispersion curves we can now proceed to calculate the interatomic force constants. These will give us some indication of the general forces between the atoms in the lattice. We should remember that we are dealing with a metal and hence the force constants are inadequate in that they do not take into account the free electrons and their screening

effects. The measured frequencies have been analyzed using Born-von Kármán models having different numbers of nearest neighbours. The elastic constants of Macfarlane and Rayne have been included in these fits. They enter the calculations with roughly the same weights as the low frequency phonons. The methods used in all these calculations are described by Svensson et al. (1965). The computer programs used were theirs.

As we said in Chapter I there is not sufficient orthogonal information in the symmetry directions of an f.c.c. lattice to work out anything more complicated than a fourth nearest neighbour model. In order to include more neighbours in the fitting process we must impose axially symmetric constraints on some of the long range force constants (Brockhouse et. al., 1967). There are two constraints required for a six neighbour model and four for an eight neighbour model. These constraint equations are given at the end of Table II-3.

When no constraints are used and forces extending to fourth neighbours are considered a quite reasonable fit is obtained. In Fig. II-4 the fitting error (which is a statistical estimate of the goodness of fit) is plotted against the number of neighbours used in the fit. We see that it drops significantly to fourth neighbours and hardly at all beyond that. The only branch that is not well fitted by a fourth neighbour model is the $[0\zeta\zeta]T_1$ branch. The inclusion of more distant neighbours improves this fit. Of course we expect this, since increasing the number of neighbours merely increases the number of Fourier coefficients which will make it easier to fit

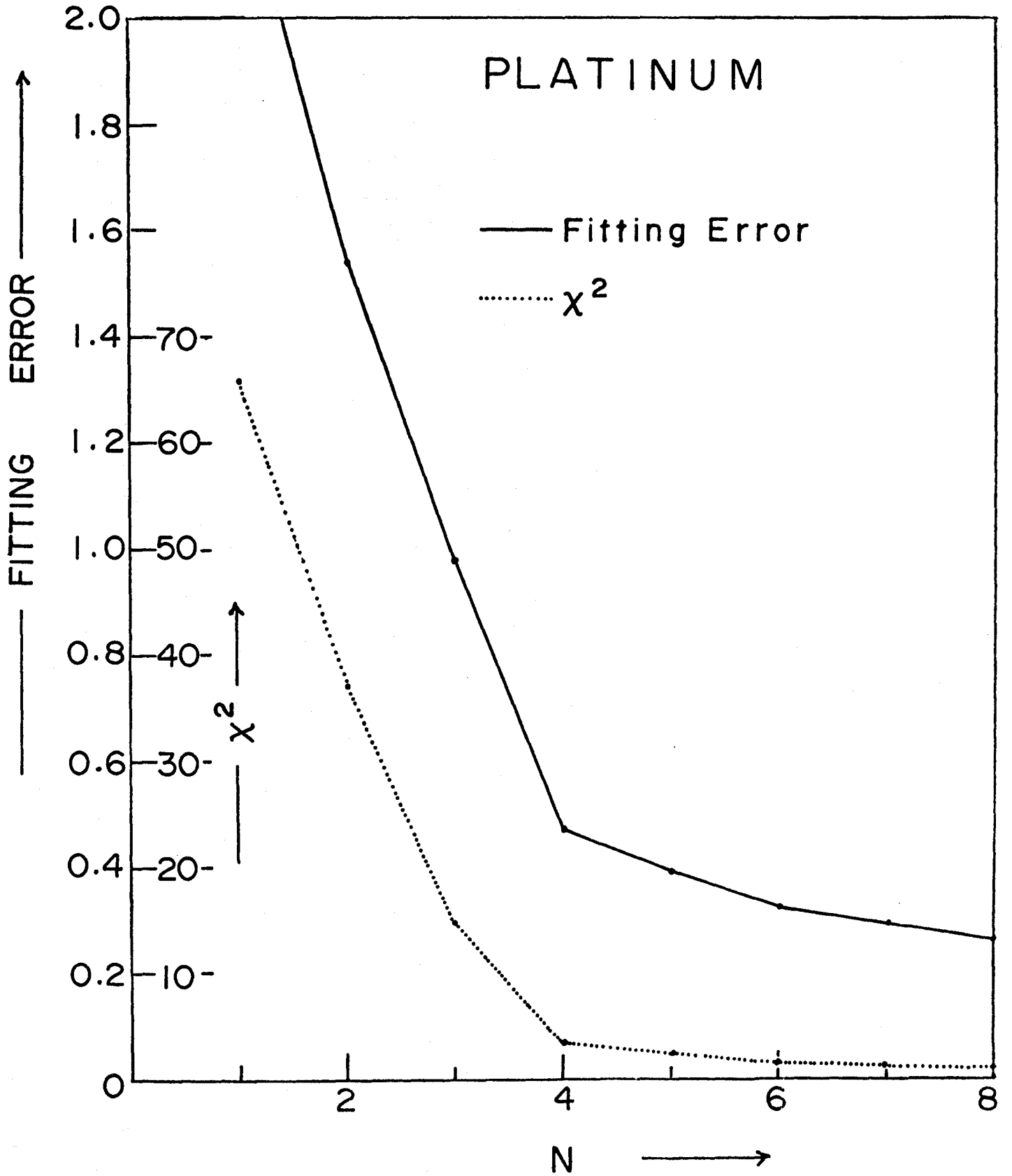

Figure II-4: The fitting error of a Born-von Kármán model as a function of the number of neighbours included in the model. Both the fitting error and the quantity χ^2 are statistical estimates of goodness of fit.

any non-smooth curve.

A sixth neighbour model fits all the branches (including the $[0\zeta\zeta]T_1$ branch) quite nicely. The use of more neighbours gives a better mathematical fit to the data but the errors on the long range force constants become so large that one cannot assign any physical meaning to the force constants themselves. The force constants calculated for fourth, sixth, and eighth neighbour models are given in Table II-3. The errors, which are calculated from the errors assigned to the frequencies, are shown in brackets.

After inspecting these force constants we may conclude that the forces out to fourth neighbours are relatively strong with first neighbour forces being far and away the most dominant. Beyond this there are weaker long range forces extending to at least sixth neighbours. There is one aspect of these force constants which is a little unusual and which will bear some discussion. In all three of the models the fourth neighbour force constants 4XX and 4XY are unusually large. In Table II-4 the force constants for Born-von Kármán models of Platinum, Palladium, Nickel, Copper and Silver are compared. Nickel lies in the same group of the periodic table of the elements as Palladium and Platinum. Copper is immediately adjacent to Nickel as is Silver to Palladium. In Nickel and Copper 4XX and 4XY are $\sim$4 or 500 dynes/cm. In Silver they are only of the order of 100 dynes/cm. In both Palladium and Platinum they are very much larger. This irregularity appearing in both these metals might well stem from the anomalous behaviour

Table II-3: Atomic force constants (units of dynes/cm.) for three Born-von Kármán models of Platinum.

AFC	4 NEIGHBOURS	6 NEIGHBOURS	8 NEIGHBOURS
1XX	25727 [150]	25886 [155]	26358 [348]
1ZZ	-7795 [206]	-7061 [216]	-7168 [494]
1XY	30675 [281]	29967 [300]	30353 [490]
2XX	5821 [275]	4027 [323]	4708 [430]
2YY	-1364 [163]	-891 [177]	-567 [190]
3XX	2629 [93]	1706 [139]	1861 [381]
3YY	105 [80]	240 [94]	16 [227]
3YZ	1657 [94]	869 [172]	1212 [201]
3XZ	1406 [59]	1345 [63]	1014 [115]
4XX	-1976 [76]	-2490 [92]	-2663 [103]
4ZZ	397 [118]	-376 [161]	-238 [203]
4XY	-3318 [111]	-2564 [195]	-2691 [510]
5XX		651 [75]	24 [323]
5YY		30 [22]	-34 [139]
5ZZ		-47 [25]	-36 [190]
5XY		232 [28]	4 [165]
6XX		422 [79]	244 [113]
6YZ		-198 [105]	-474 [172]
7XX			240 [163]
7YY			-52 [195]
7ZZ			110 [53]
7YZ			59 [19]
7XZ			89 [28]
7XY			177 [50]
8XX			548 [120]
8YY			-87 [86]

Constraint Equations

1) 9(5YY)-(5XX)-8(5ZZ)=0
2) 3(5XX)-3(5YY)-8(5XY)=0
3) 3(7YZ)-(7XY)=0
4) 2(7XZ)-(7XY)=0

Force Constant Matrix

$$\begin{pmatrix} nXX & nXY & nXZ \\ nXY & nYY & nYZ \\ nXZ & nYZ & nZZ \end{pmatrix}$$

Table II-4: A comparison of atomic force constants (units of dynes/cm.) in Pt,Pd,Ag,Cu and Ni.

AFC	Pt.	Pd.	Ag.	Cu.	Ni.
1XX	26358	19337	10808	13160	17319
1ZZ	-7168	-2832	-1815	-1489	-436
1XY	30353	22423	12394	14880	19100
2XX	4708	1424	506	453	1044
2YY	-567	210	-340	-345	-780
3XX	1861	744	546	573	842
3YY	16	249	247	321	263
3YZ	1212	163	322	252	-109
3XZ	1014	708	262	342	424
4XX	-2663	-1142	-22	99	402
4ZZ	-238	-223	63	-190	-185
4XY	-2691	-1370	156	424	660
5XX	24	-6	-155	-121	-85
5YY	-34	-207	-60	15	7
5ZZ	-36	-232	-47	32	18
5XY	4	76	-36	-51	-35
6XX	244	154	-105	-111	
6YZ	-474	330	-362	-337	
7XX	240	70	15	31	
7YY	-52	67	-2	39	
7ZZ	110	-20	-36	-89	
7YZ	59	-22		9	
7XZ	89	-32	22	13	
7XY	177	-65	44	26	
8XX	548	72	-39	-201	
8YY	-87	6	176	54	

of the T_1 branches. We will shortly attempt to establish whether it does or not. For the moment we will assume it normal and proceed to calculate a frequency distribution. The sixth neighbour model seems the most realistic so we will use the force constants derived from that model as our starting point.

These force constants can now be used to calculate frequencies for any wave vector ($\vec{q}$) in reciprocal space. If enough of these frequencies are calculated they can be sorted into channels of some given width in frequency and the number of frequencies in each channel can be established. This will give a distribution of frequencies $g(\nu)$ which can be used in calculating thermodynamic properties as we shall see. A direct method of calculation, involving diagonalization of a 3 x 3 matrix for each point in reciprocal space, is too time consuming. Various methods of approximation have been developed. Here we have used the method of Gilat and Raubenheimer (1966) in which frequencies are calculated directly at only a limited number of points in $\vec{q}$-space while the other necessary frequencies are obtained by interpolating between these calculated points. We should perhaps point out that because of the symmetry of the crystal these calculations need only be performed in the irreducible 1/48 th symmetry element of the first Brillouin zone.

The resultant frequency distribution is shown in Fig. II-5. The calculations were performed with a bin width of 0.01×10^{12} cps. The smooth curve in the figure was drawn through the cal-

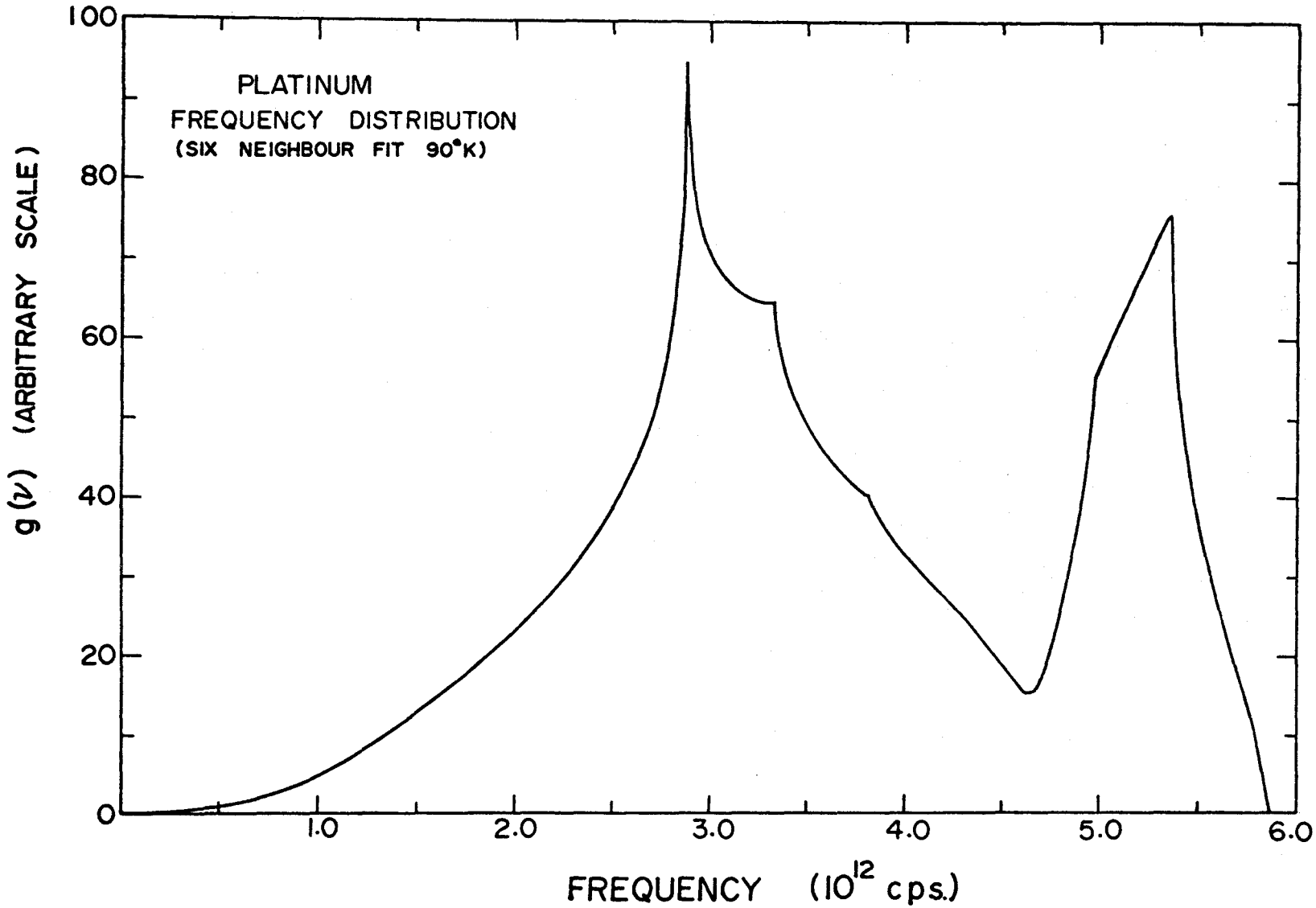

Figure II-5: The distribution of frequencies in Platinum at 90°K calculated from a six neighbour Born-von Kármán model.

culated histogram. The critical points in this distribution can all be correlated with the stationary values and cross over points of the dispersion curves. We should note here that all the frequencies are calculated using force constants derived by fitting measurements in the symmetry directions only. We are assuming that the model is sufficient to yield correct values for the frequencies at off-symmetry points in reciprocal space. Strictly speaking we should go and measure some off-symmetry points and see if the force constants predict accurately the frequencies at those points. However this has been done for both Palladium and Copper (Miiller, 1969) and there the models do predict the correct frequencies, on the average. It was not thought necessary to repeat this process here.

As a check on our frequency distribution we can use it to calculate the specific heat as a function of temperature. However in doing this we assume that the frequencies (and hence $g(\nu)$) are independent of temperature. This is not so and in order to get any decent values for the specific heat, especially at high temperatures one must use a more sophisticated approach than the Harmonic approximation. However, for temperatures less than 100°K or so values calculated in this approximation should agree with the measured values. If they do not then something is wrong with the force model. So what we are about to do provides us with a check on our model.

In the harmonic approximation the total internal energy may be written as

$$E = \int_0^{\nu_m} \frac{h\nu\, g(\nu)\, d\nu}{[\exp(\beta h\nu) - 1]} \qquad \text{II-1}$$

where ν_m = the maximum frequency of the crystal

$\beta = 1/kT$

k = the **Boltzmann factor**

T = the temperature.

$g(\nu)$ must be normalized to the total number of modes of oscillation, i.e.

$$\int_0^{\nu_m} g(\nu)\, d\nu = 3N \qquad \text{II-2}$$

Then the specific heat at constant volume is given by

$$C_v = \left[\frac{\partial E}{\partial T}\right]_v = k \int_0^{\nu_m} \frac{(\beta h\nu)^2 \exp(\beta h\nu)\, g(\nu)\, d\nu}{[\exp(\beta h\nu - 1)]^2} \qquad \text{II-3}$$

These calculations have been done using the $g(\nu)$ obtained at 90°K. C_v is plotted as a function of temperature in Fig. II-6. Shown also are the measured values of C_p (specific heat at constant pressure) which have been compiled by Hultgren et. al. (1963). Below 100°K the agreement is very good. It would seem that there is nothing drastically wrong with our model within the limits of the Harmonic approximation.

Let us leave this for now and return to a discussion of the force constants. We noticed that the fourth neighbour terms 4XX and 4XY were unusually large. Since this behaviour is common to both Palladium and Platinum it might well be related to the anomalies in the T_1 branches. So far we have paid scant attention to these. Let us now remove them completely and replace the anomalous branch by a smooth curve. Then we can

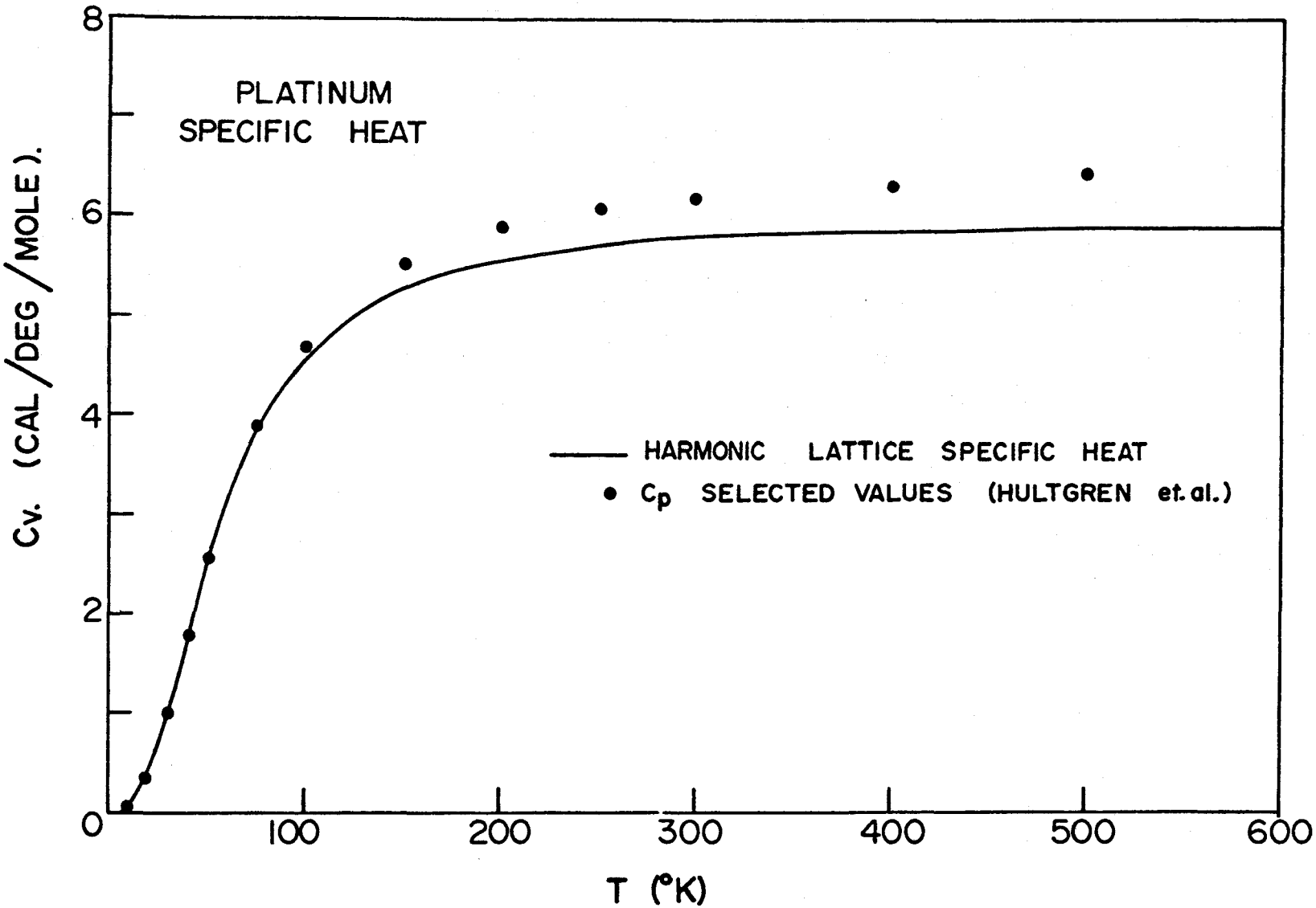

Figure II-6: The lattice specific heat of Platinum calculated from the frequency distribution of Fig.II-5.

recalculate the force constants and see whether 4XX and 4XY still remain large.

We know (see Chapter I) that any symmetry branch can be fitted by an expansion in terms of the interplanar force constants

$$M\omega^2 = \sum_n \phi_n(1-\cos(n\pi q/q_m)) \qquad \text{II-4}$$

In most f.c.c. metals (Ni, Cu, Ag) the T_1 branch can be well fitted using only the first two terms of the expansion. With some manipulation the equation becomes

$$\nu^2 = A_1[\sin^2(\tfrac{\pi\zeta}{2}) + A_2/A_1 \sin^2(\pi\zeta)] \qquad \text{II-5}$$

where $\nu = \omega/2\pi$ = frequency

and $A_2/A_1 = \phi_2/\phi_1$

A_1 may be fixed by assuming the frequency measured at the zone boundary to be beyond the region of the anomaly. This is a safe assumption since the frequency is identical to that observed at the zone boundary in the [00ζ] direction where no anomaly was found. Now a value for A_2/A_1 may be chosen and frequencies calculated for the same values of ζ as were measured. This pseudo-T_1 branch is then fitted to the other measured frequencies using a Born-von Kármán model. The value of A_2/A_1 finally used is that which gives the minimum fitting error. The value finally chosen was $A_2/A_1 = 0.09$.

Now we have a smooth T_1 branch which is as much in tune with the other branches as we can make it. We again consider the force constants. Table II-5 shows that they are not significantly changed from their previous values. In particular 4XX and 4XY are still overly large. We may therefore conclude that the odd values of these force constants do not originate solely

Table II-5: Atomic force constants(units of dynes/cm.) for Platinum at 90°K when the anomalous T_1 branch is replaced by a smooth curve.

AFC	4 NEIGHBOURS	6 NEIGHBOURS	8 NEIGHBOURS
1XX	26243 [154]	26325 [165]	26168 [350]
1ZZ	-7331 [211]	-7171 [217]	-6773 [495]
1XY	29913 [286]	29405 [306]	29616 [491]
2XX	5706 [277]	4961 [342]	5537 [433]
2YY	-847 [167]	-851 [179]	-686 [191]
3XX	1937 [108]	1833 [140]	1628 [382]
3YY	203 [82]	119 [100]	246 [230]
3YZ	881 [102]	702 [178]	639 [202]
3XZ	1131 [63]	1153 [68]	1015 [121]
4XX	-2426 [85]	-2573 [93]	-2638 [104]
4ZZ	567 [130]	298 [169]	65 [208]
4XY	-2577 [139]	-1943 [202]	-2011 [514]
5XX		219 [94]	142 [325]
5YY		72 [26]	-137 [140]
5ZZ		54 [31]	-172 [190]
5XY		55 [36]	105 [165]
6XX		180 [86]	2 [114]
6YZ		-194 [117]	39 [180]
7XX			54 [171]
7YY			110 [196]
7ZZ			75 [53]
7Y			-6 [22]
7XZ			-10 [32]
7XY			-19 [59]
8XX			221 [146]
8YY			100 [118]

in the anomalous behaviour of the T_1 branch.

To sum up we may say that the force system of Platinum seems adequately described by a sixth neighbour Born-von Kármán model. First neighbour forces are dominant but relatively large forces exist out to fourth neighbours. The longer range forces are much weaker. These conclusions are supported by the good fit obtained to the dispersion curves and by the good agreement of calculated and measured specific heats in the harmonic region ($T \sim 100°K$). The unusual values of the fourth neighbour force constants do not appear to be related to the anomalous behaviour of the T_1 branch. The detailed consideration of this behaviour is the subject of the next chapter.

CHAPTER III

ANOMALOUS LATTICE VIBRATIONS IN PALLADIUM AND PLATINUM

1. Introduction

It was pointed out in Chapter I that the present work was provoked by Miller's discovery of anomalous behaviour in Palladium. There was a pronounced increase in slope in the $[0\zeta\zeta]T_1$ branch of the dispersion curves, with a much smaller possible effect in the $[\zeta\zeta\zeta]T$ branch. The effect was very broad and it was difficult to say where it began and ended. Measurements made at temperatures of 8, 90, 120, 296, 673 and 853°K demonstrated that the anomaly weakened and eventually disappeared as the temperature was increased.

For various reasons the possibility of the anomaly being a Kohn effect (see next section) was dismissed. Firstly the Kohn effect is expected to manifest itself as a sharp singularity in the dispersion curves. The observed effect was not sharp. Secondly the Kohn effect is not expected to depend strongly on temperature (at least for temperatures as far below the melting point as these were). Thirdly initial attempts to find Kohn vectors which would account for the anomaly were not successful. There were two Kohn surfaces which crossed the $[0\zeta\zeta]$ direction at $\zeta\simeq0.4$ but the anomaly seemed to be centred at $\zeta\simeq0.35$. Initially it was thought that the Kohn anomaly, if it was present at all, would only modulate the shape of the principle anomaly.

Another possibility that was considered and dismissed was that impurities in the Palladium crystal were causing the

effect. Palladium will become ferromagnetic if sufficient magnetic impurities are added to it. However a spectrographic analysis of a piece of the crystal revealed that the amount of magnetic impurities in the sample was an order of magnitude less than the amount required to make Palladium magnetic.

This was the state of affairs at the time the present measurements were commenced. A number of lines of attack have been pursued. Firstly, to ensure that impurity effects were not important, a second crystal of very pure Palladium was procured and the measurements in the T_1 branch repeated. Secondly measurements were made in certain off-symmetry directions in Palladium to determine the extent of the anomaly. In addition the T_2 branch was thoroughly measured at 90°K. Thirdly it was decided to investigate Platinum since it lies in the same group of the period table as Palladium. Lastly the T_1 branch of Nickel was measured at 90°K since Nickel also lies in this group.

The result of all this endeavour has been the resurrection of the Kohn effect explanation. Though detailed calculations are very difficult to make a qualitative analysis indicates that this is the cause of the anomalies in both Palladium and Platinum. Before proceeding to describe the measurements let us briefly discuss the Kohn effect.

2. The Kohn Effect

In Chapter I we discussed the validity of the Adiabatic approximation in metals. We cited the calculations of Ziman (1964) and Cochran (1965) as showing that an ion and its electronic

screening charge could be treated as a neutral pseudo-atom which can be used in Born-von Kármán models. In these calculations one considers the effect of introducing a small charge distribution into a gas of free electrons. The electrons will attempt to screen this charge distribution and some interaction potential $V_s(\vec{k})$ will result. This potential is inversely proportional to a dielectric function $\varepsilon(\vec{k})$ defined as

$$\varepsilon(\vec{k}) = 1 + \frac{6\pi Ne^2}{k^2 E_F}\left\{\frac{1}{2} + \frac{4k_F^2 - k^2}{8k_f k}\ln\left|\frac{2\vec{k}_f + \vec{k}}{2\vec{k}_f - \vec{k}}\right|\right\} \qquad \text{III-1}$$

where N = the number of free electrons

$\vec{k}$ = some wave vector

$E_f, \vec{k}_f$ = the Fermi energy and wave vector respectively (divided by $\hbar$)

From this expression we see that there will be some logarithmic singularity at $\vec{k} = 2\vec{k}_F$. The resultant discontinuity in $V_s(\vec{k})$ means that the forces between the pseudo-atoms must change. Hence we would expect some sort of discontinuity in the dispersion curves at this wave vector. The physical reason for this behaviour is that the electrons all have wave vectors less than $\vec{k}_F$ (by definition of the Fermi surface). If $\vec{k}$ becomes greater than $2\vec{k}_F$ the electrons can no longer screen the ions effectively and hence the forces between the ions will change substantially at $\vec{k} = 2\vec{k}_f$. Therefore the frequencies of oscillation must change. The resultant kink in the dispersion curves is called the Kohn effect (Kohn, 1959). Because the Fermi surface in metals is relatively sharp we would expect a sharp discontinuity

in the dispersion curves.

Of course the Fermi surface in most metals is not spherical. The above results can be generalized so that a Kohn effect will occur whenever the momentum transfer $\vec{Q}$ is

$$\vec{Q} = \vec{k}_2 - \vec{k}_1 \qquad \text{III-2}$$

where $\vec{k}_2$ and $\vec{k}_1$ are any two points on the Fermi surface having parallel tangents. Given the Fermi surface it is not difficult to sort out vectors across the surface which should yield Kohn effects in the symmetry directions. What is difficult is to calculate the magnitude of any such effect. We will not attempt to do this here. Our analysis will be concerned with establishing the possible positions of Kohn anomalies.

3. Experimental Results

The $[0\zeta\zeta]T_1$ Branch of Platinum

Frequencies were measured at closely spaced points along the $[0\zeta\zeta]T_1$ branch under the conditions of high resolution described in Chapter II. More widely spaced measurements were made at a different incident frequency of 9.03×10^{12} cps. These latter results are in good agreement with the high resolution measurements. A list of frequencies measured at three temperatures is given in Table III-1. The T_1 branch of Platinum at 90°K is compared to that of Palladium at 8°K in the upper part of Fig. III-1. The solid symbols represent those measurements made with vertical collimation and an incident frequency of 7.02×10^{12} cps.; the open squares those with the same incident energy but no vertical collimation. The open triangles represent measurements made with higher incident energies. The slopes of

Table III-1: Normal mode frequencies in the T_1 branch of Platinum at 90,296 and 473°K.

	90 K	296 K	473 K
0.100	0.580 (0.02)	0.510 (0.02)	0.495 (0.02)
0.125		0.660 (0.02)	0.635 (0.02)
0.150	0.835 (0.02)	0.780 (0.02)	0.750 (0.02)
0.175		0.900 (0.02)	0.860 (0.02)
0.200	1.050 (0.02)	1.005 (0.02)	0.970 (0.02)
0.225		1.125 (0.02)	1.085 (0.02)
0.250	1.255 (0.02)	1.210 (0.02)	1.180 (0.02)
0.275	1.345 (0.02)	1.300 (0.02)	1.270 (0.02)
0.300	1.430 (0.02)	1.390 (0.02)	1.375 (0.02)
0.325	1.510 (0.03)	1.485 (0.02)	1.470 (0.02)
0.350	1.540 (0.03)	1.570 (0.02)	1.560 (0.02)
0.375	1.650 (0.03)	1.665 (0.02)	1.670 (0.02)
0.400	1.770 (0.03)	1.775 (0.02)	1.780 (0.02)
0.425	1.895 (0.02)	1.900 (0.02)	1.900 (0.02)
0.450	2.020 (0.02)	2.025 (0.02)	2.045 (0.02)
0.475		2.165 (0.02)	2.155 (0.02)
0.500	2.255 (0.02)	2.290 (0.02)	2.275 (0.02)
0.525		2.400 (0.02)	2.390 (0.02)
0.550	2.510 (0.02)	2.530 (0.02)	2.515 (0.02)
0.575		2.660 (0.02)	2.620 (0.02)
0.600	2.810 (0.02)	2.780 (0.02)	2.750 (0.02)
0.625			2.860 (0.02)
0.650	3.080 (0.02)	3.025 (0.02)	
0.700	3.27 (0.03)	3.230 (0.02)	
0.800	3.57 (0.03)		
0.900	3.76 (0.04)		
1.000	3.84 (0.05)		

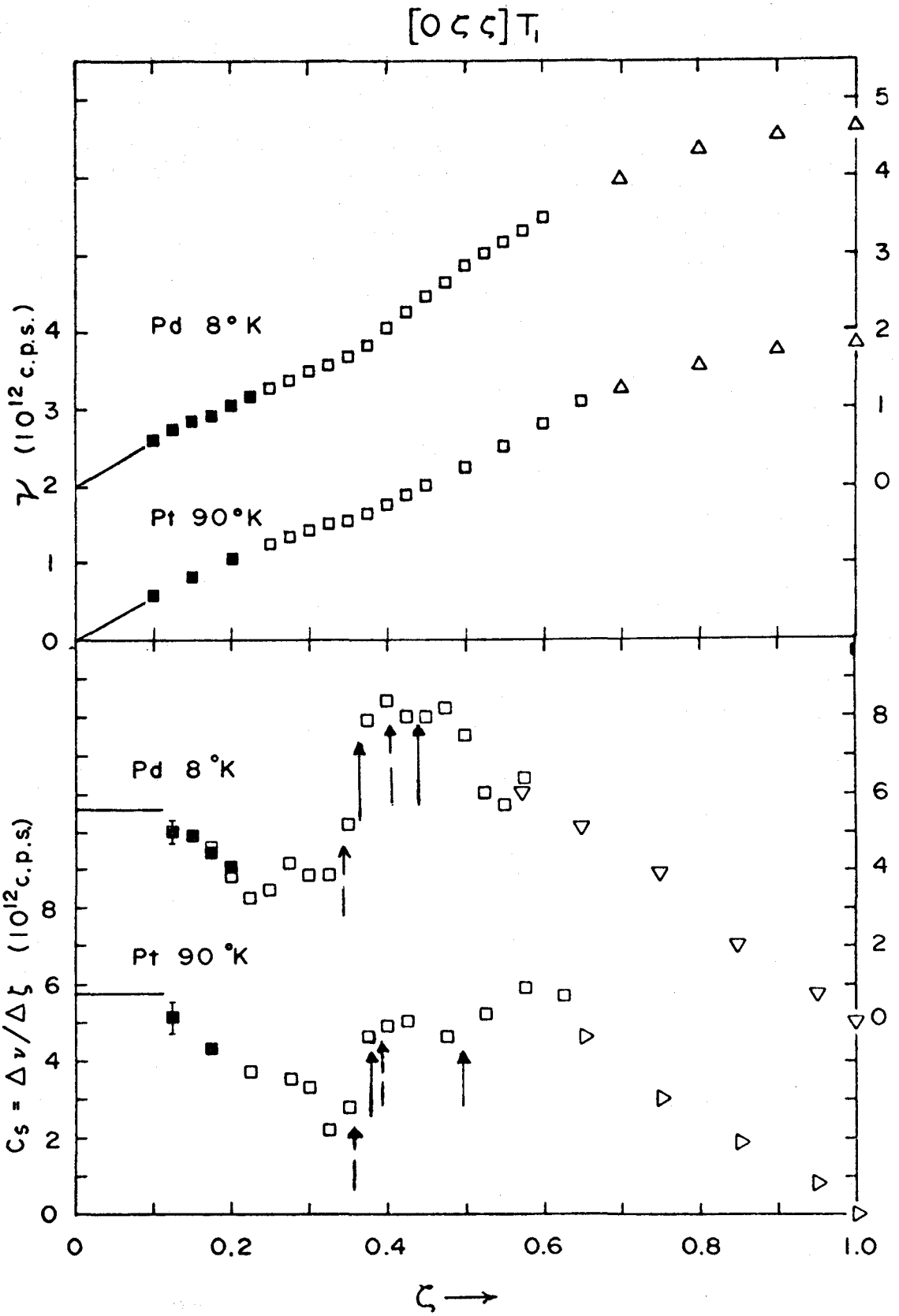

Figure III-1: The T_1 branches of Palladium and Platinum. The upper half of the picture shows the dispersion curves while the lower half shows the slopes of these curves. The various symbols are explained in the text.

the solid straight lines are the velocities of sound described in the last chapter.

The lower part of Fig. III-1 shows the slopes of the two dispersion curves plotted as a function of ζ. This type of plot gives a much more graphic representation of the anomalous behaviour than do the dispersion curves themselves. The various symbols have the same meanings as those in the upper part of the diagram. The arrows in the figure will be explained shortly.

Thorough measurements along the other transverse branches did not indicate any more anomalous behaviour except possibly in the $[0\zeta\zeta]T_2$ branch. There does seem to be some small effect in this branch but the measurements were made at two different incident energies and it is difficult to compare them accurately enough to define the behaviour.

The work described above was done at 90°K. The T_1 branch has also been measured at 296 and 473°K under the same experimental conditions. The results are shown in Fig. III-2. Table III-1 gives a list of the frequencies. The anomaly is seen to weaken at higher temperatures in much the same way as in Palladium

Anomalous Behaviour in Palladium

The second crystal of Palladium was used to remeasure the T_1 branch at a temperature of 296°K. This crystal was about half the size of the original one, being a cylindrical boule of length 2" and diameter 1/4". A [100] axis lay along the axis of the cylinder which made the geometrical arrangement very

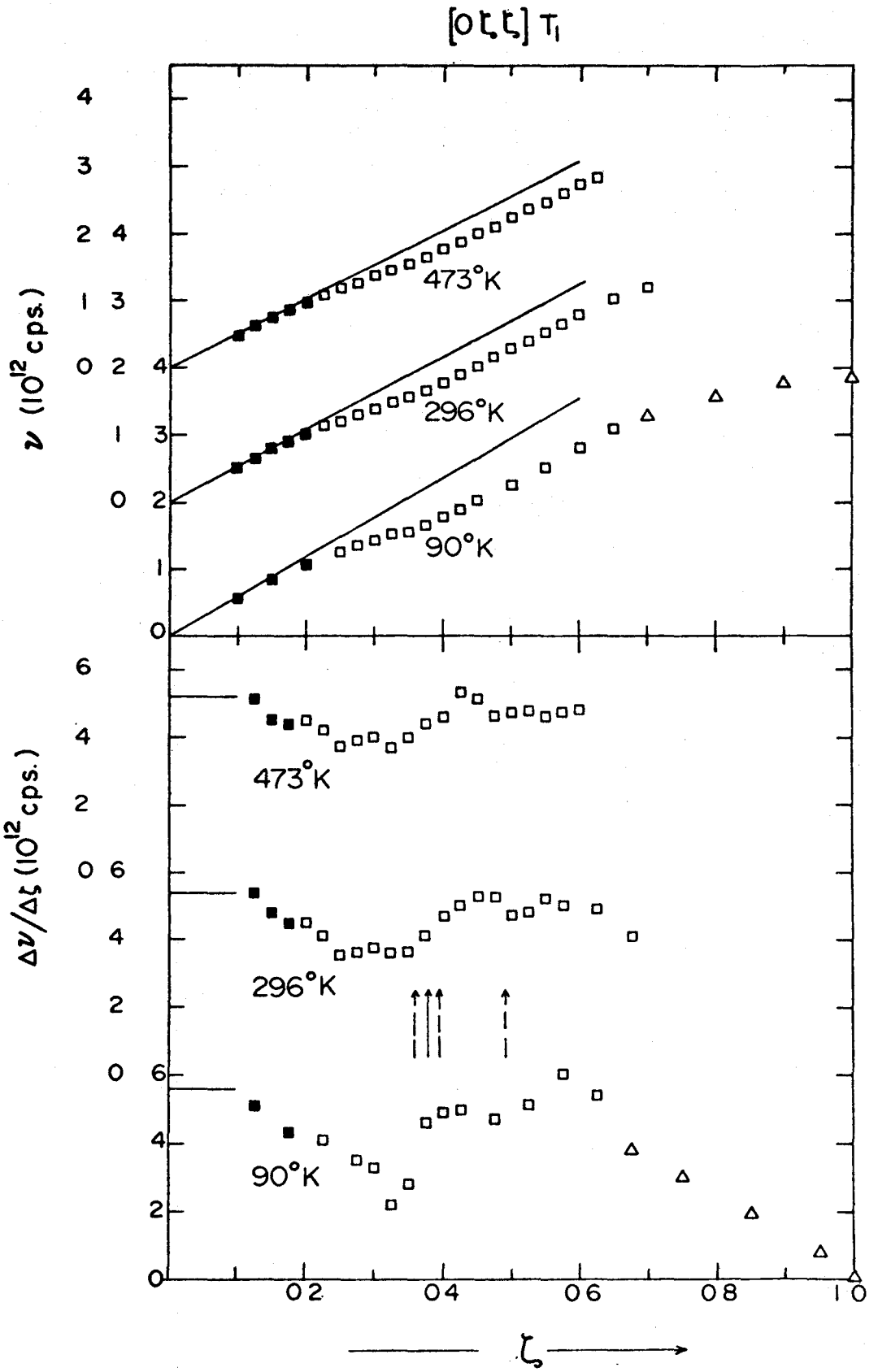

Figure III-2: The temperature dependence of the T_1 branch of Platinum. The arrows in the lower half of the diagram indicate the positions of possible Kohn vectors.

good for measurements in the (100) plane. These measurements were made under the same conditions as Miiller's earlier work. The results are shown in Fig. III-3 where they are compared to Miiller's measurements. The anomaly occurs in exactly the same way as before.

The extent of the anomaly has been measured in the (100) plane of the original Palladium crystal. Measurements were made along directions making angles θ = 7.5, 15, 22.5, 30 and 37.5° with the [0ζζ] axis. Along each of these directions it was thought necessary to go out a distance equal to 0.6 of the distance between reciprocal lattice points in the [0ζζ] direction. Most of the work was done at 90°K, the only exception being in the direction θ = 15°. This was done at 8°K by Dr. Miiller. All the measurements were made at an incident frequency of 7.02×10^{12} cps. A list of the frequencies in these directions is given in Table III-2. The slopes of these dispersion curves are shown in Fig. III-4. We can see that the anomaly has petered out by θ = 30°. In the [00ζ] direction (θ=45°) there is of course no effect.

Such off-symmetry measurements were not made in Platinum since it was thought that the results would be very similar to those in Palladium.

The $(0\zeta\zeta)T_2$ branch of Palladium was not measured in great detail by Miiller. In the present work measurements were made at intervals of 0.025 in ζ. This work was done at a temperature of 90°K using an incident frequency of 11.04×10^{12} cps. The curve and its slopes are presented in Fig. III-5.

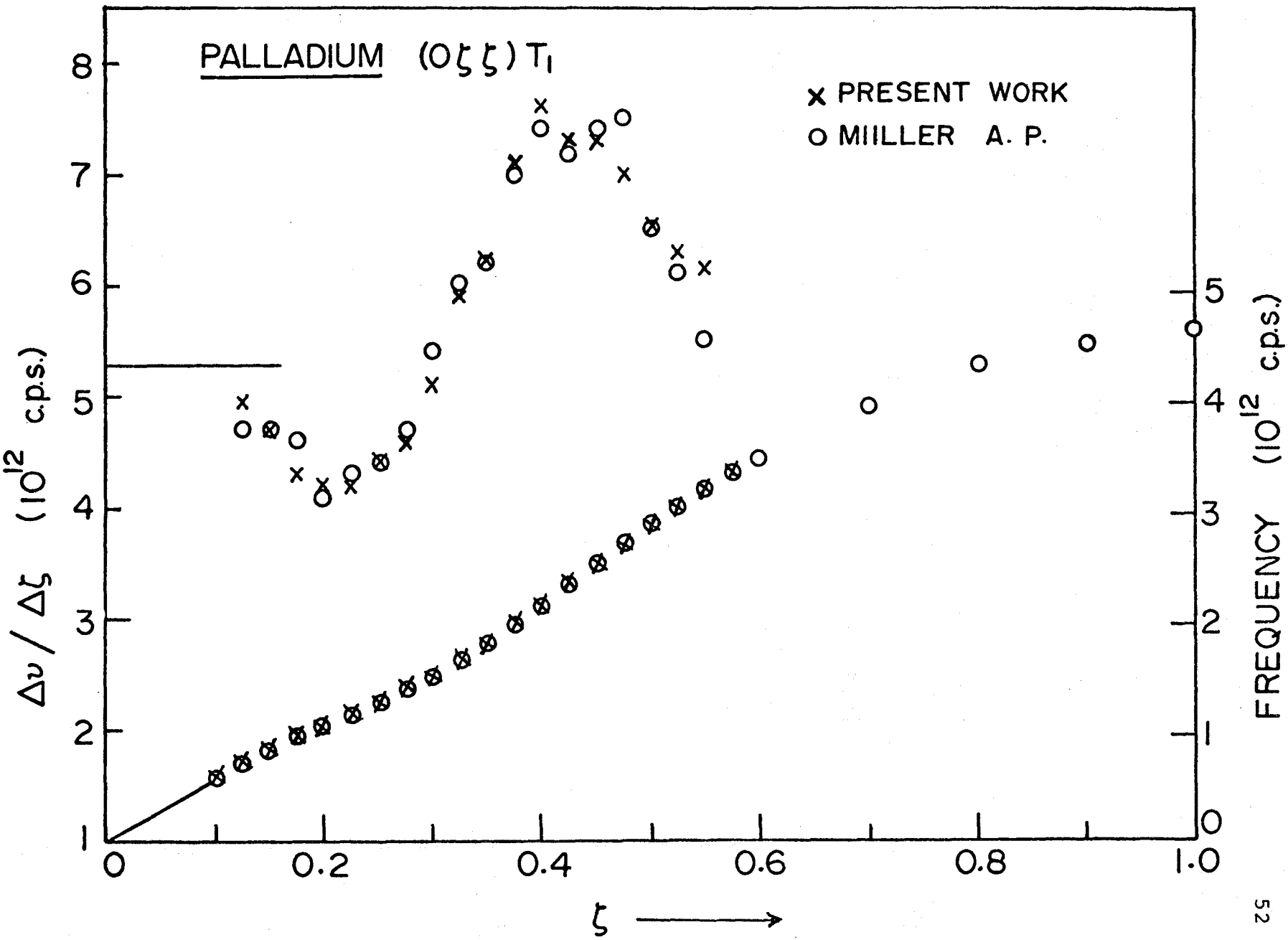

Figure III-3: The T_1 branch of Palladium comparing the results of Miiller to those of the present work.

Table III-2: Normal mode frequencies (units of 10^{12} cps.) in off-symmetry directions in the (100) plane of Palladium.

	θ = angle from [110] direction			
ζ	7.5	15.0	22.5	30.0
0.075	0.500			0.640
0.100	0.615	0.685	0.740	0.865
0.125	0.770	0.835	0.915	1.045
0.150	0.890	0.980	1.075	1.270
0.175	1.020	1.140	1.262	1.425
0.200	1.120	1.295	1.400	1.600
0.225	1.245	1.420	1.575	1.800
0.250	1.310	1.520	1.700	1.990
0.275	1.405	1.620	1.900	2.180
0.300	1.500	1.795	2.045	2.360
0.325	1.685	1.950	2.225	
0.350	1.835	2.140	2.405	2.730
0.375	2.025	2.265	2.580	
0.400	2.150	2.465	2.775	3.110
0.425	2.355	2.605	2.950	
0.450	2.515	2.785	3.150	3.487
0.475	2.690	2.905	3.305	
0.500	2.865	3.105	3.475	
0.525	3.055	3.230		
0.550	3.215	3.430		
0.575	3.380	3.570		
0.600	3.530			

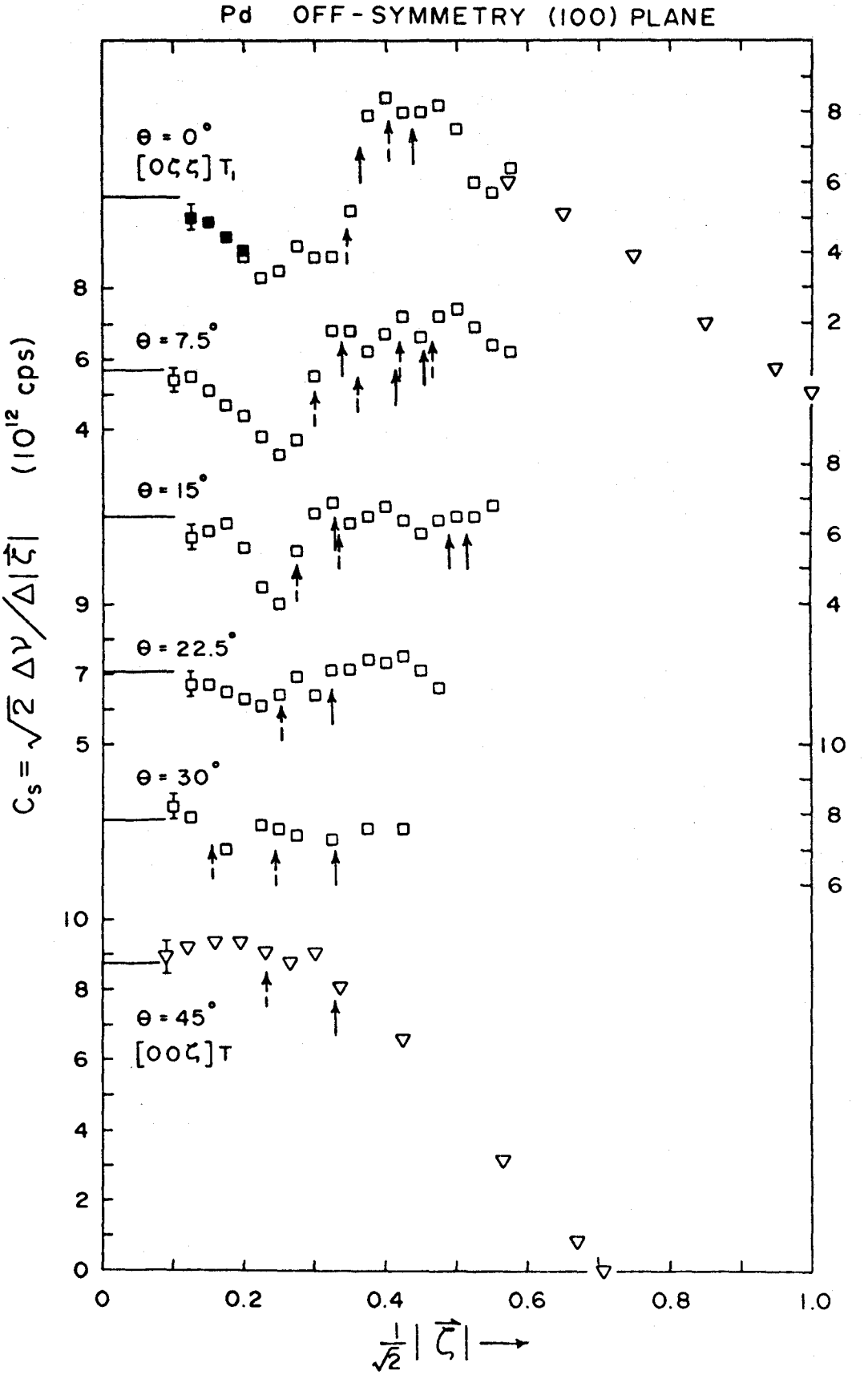

Figure III-4: The slopes of the transverse branches in the (100) plane of Platinum at angles of 7.5,15.0,22.5 and 30.0° to the [110] direction

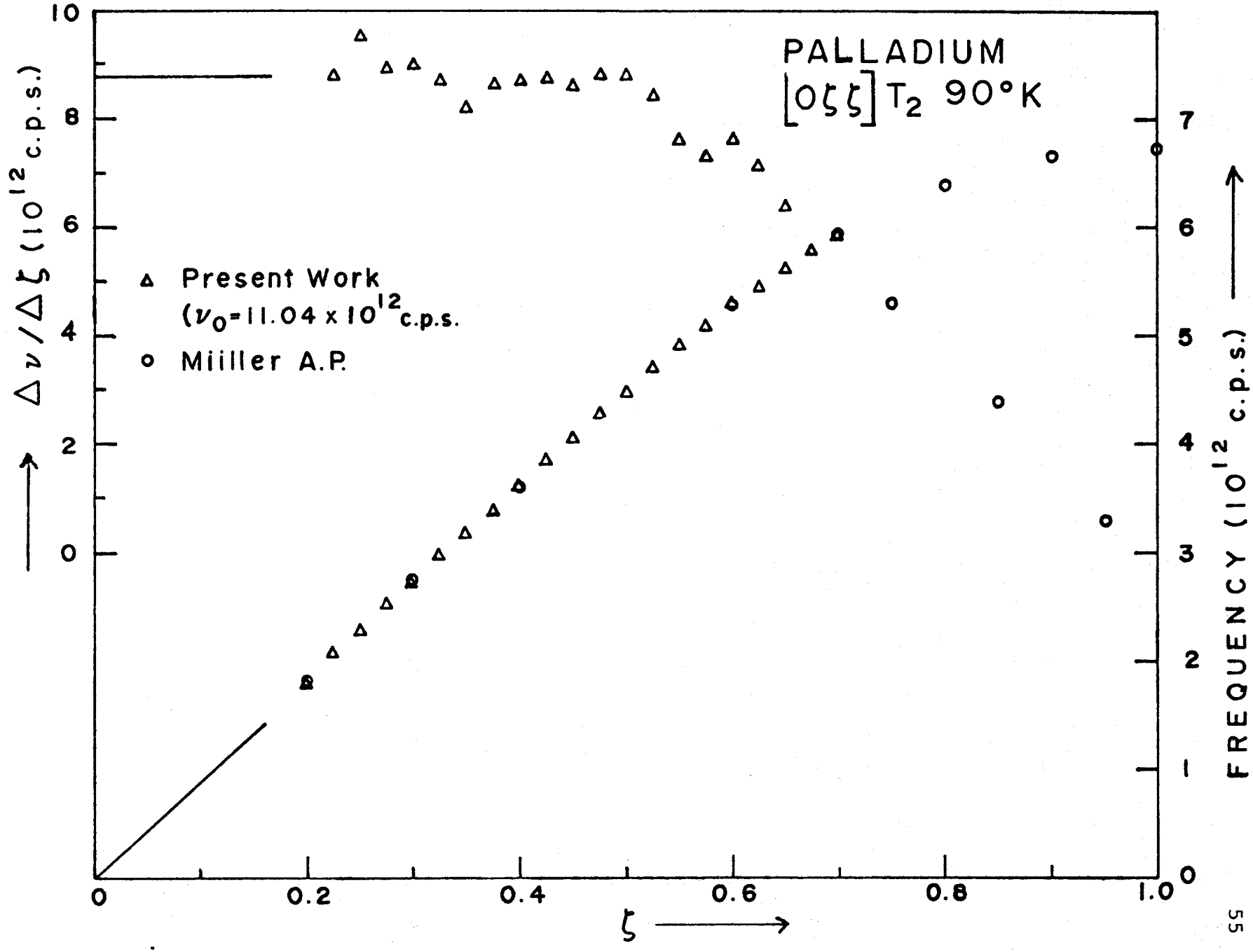

Figure III-5: The T_2 branch of Palladium at 90°K showing the dispersion curve and its slopes.

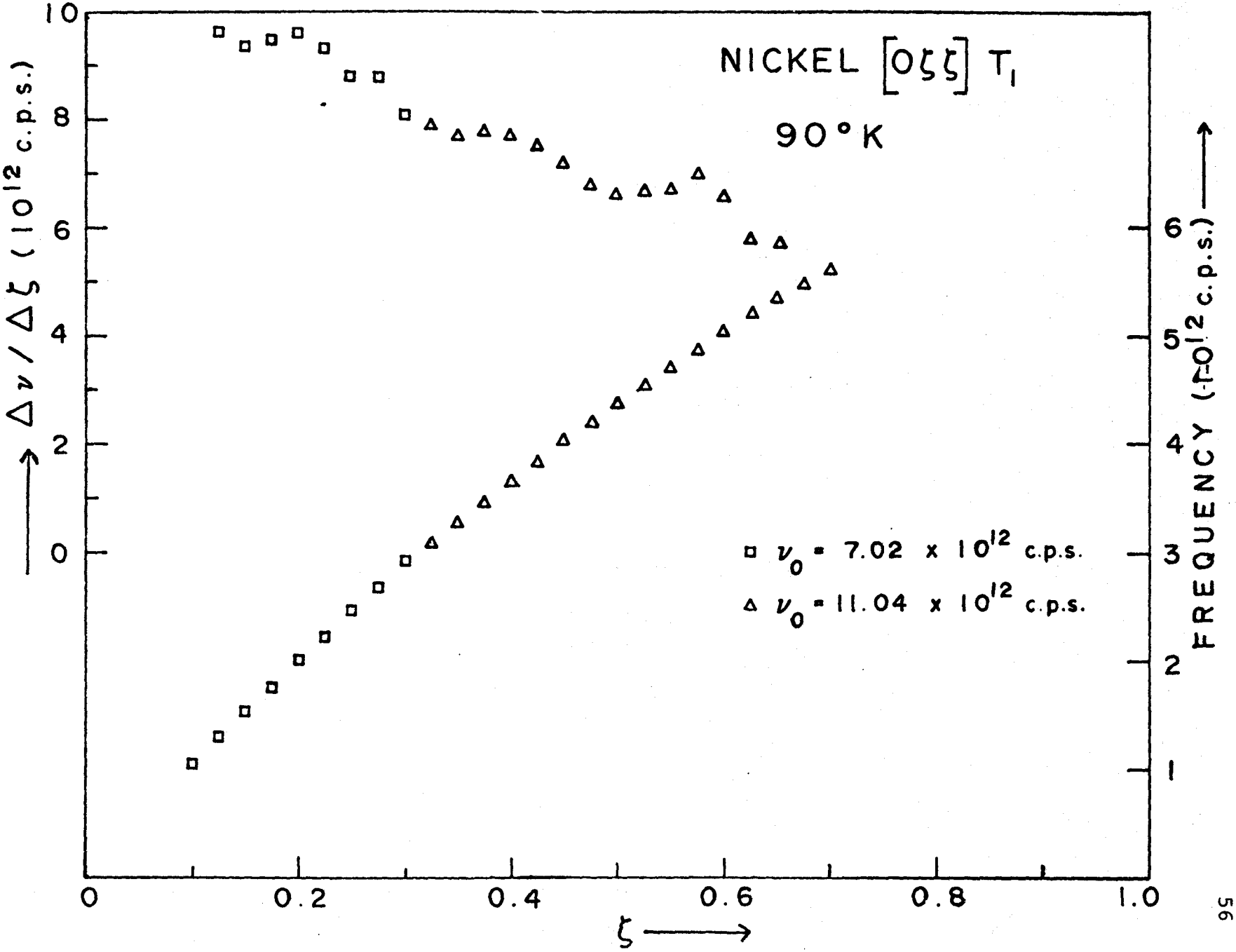

Figure III-6: The T_1 branch of Nickel at 90°K. showing the dispersion curve and its slopes.

There is no evidence of the type of anomaly seen in the T_1 branch.

The $(0\zeta\zeta)T_1$ branch of Nickel has also been measured in detail at 90°K. Incident frequencies of 11.04 and 7.02 x 10^{12} cps were used. The results are shown in Fig. III-6. There may, perhaps, be something untoward occuring but it is not the same type of behaviour as is observed in Platinum and Palladium.

4. Analysis and Discussion of Results

First we may say that we are definitely dealing with a real effect and not some by-product of impurities. That the effect should occur in two samples of Palladium and in Platinum is proof enough of this. Also it would seem likely that the anomaly does not have its origin in the nearly magnetic properties of Palladium.

Let us briefly compare the anomalies in the two metals. We can see from Fig. III-1 that the effects are not identical. For low ζ the frequencies of the T_1 branches are nearly the same. The dispersion curves begin to dip at about the same ζ. At higher values of ζ the behaviours of the two differ. In Palladium the curve bends up again, rising to the velocity of sound line before beginning to level off to the zone boundary. Platinum does not do this. Though the dispersion curve starts to rise again it does not rise as steeply as in Palladium. In fact it ends up looking as if the upper half of the curve had been displaced from the lower half along ζ.

The differences are pointed up more clearly by the slope plots of Fig. III-1. We can see that the effect in Platinum seems to extend over a wider range than it does in Palladium.

The Fermi Surface: Some Possible Kohn Anomalies

The Fermi surfaces of Platinum and Palladium have been calculated by Krogh Andersen and Mackintosh(1968) using a relativistic augmented plane wave method. The calculated surfaces are in good agreement with the extremal areas derived from the de Haas-van Alphen measurements(see Krogh Andersen and Mackintosh). The Fermi surfaces consist of three parts: 1) a Γ-centred electron surface, 2) an open, d-like hole surface having the topology of cylinders extending in the(100) direction and intersecting at the points X, 3) a set of d-like hole surfaces having the forms of ellipsoids of revolution, centred at the points X. Cross sections of these surfaces in the (100)and $(1\bar{1}0)$ planes are shown in Fig. III-7. We shall concentrate our attention on the (100) plane. In particular we shall be interested in the open hole surfaces intersecting at the points X. We can see immediately that there are numerous pairs of points on this surface having parallel tangents. Suppose that for some such pair we call the vectors from the origin (Γ) to the two points, $\vec{k}_2$ and $\vec{k}_1$. Then the set of all the vectors $\vec{k}_2-\vec{k}_1$ is the set of all possible Kohn vectors arising from this surface. If we translate all these vectors to a common origin (Γ) then their tips will form a number of loci which will be Kohn anomaly surfaces. Some of these surfaces will extend beyond the first Brillouin zone. Since in this,

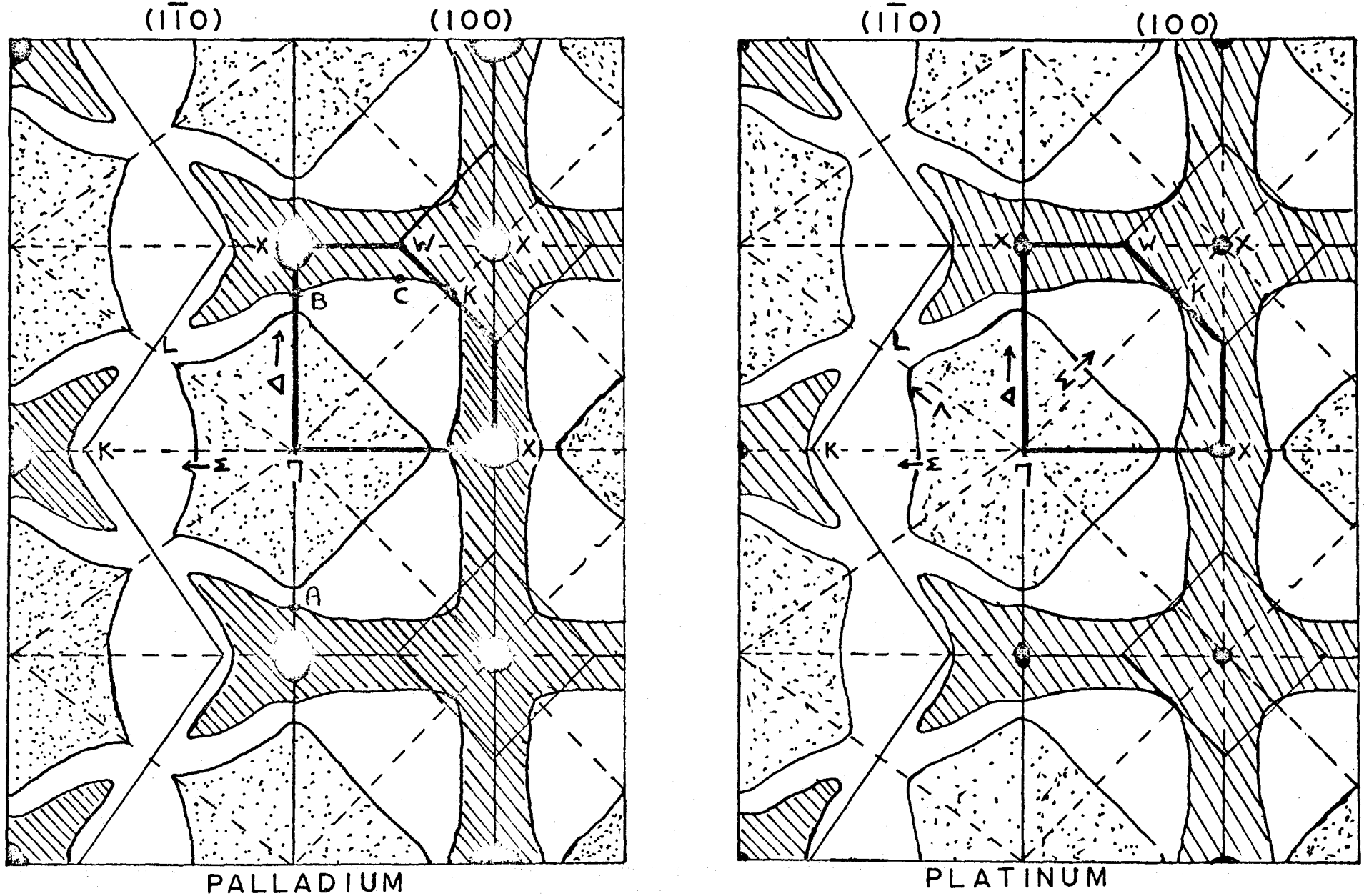

Figure III-7: Cross sections of the Fermi surfaces of Palladium and Platinum in both the (100) and (1$\bar{1}$0) planes. The quarter sections of the first Brillouin zones (heavily outlined) in the (100) planes are reproduced in Figures III-8 and III-9. The various surfaces are described in the text

as in all matters of this sort, we must maintain translational symmetry we can reflect all these surfaces back into the first zone by adding a suitable reciprocal lattice vector. This is just equivalent to mapping all the above surfaces about adjacent reciprocal lattice points.

We can use a computer to make all these calculations. First it is necessary to describe the Fermi surface mathematically in terms of a polynomial which is adjusted to fit a number of closely spaced points. After this the polynomial may be solved for points having the same slope and the vectors separating these points can be translated to the origin. When this process is repeated for the full gamut of slopes we end up tracing out the necessary Kohn surfaces. These surfaces are shown in Figs. III-8 & III-9. Note that we differentiate between equivalent and non-equivalent points on the Fermi surface. In Fig. III-7 the points A and B are equivalent while A and C are not, though all the vectors AB, AC and BC are possible Kohn vectors. Both equivalent and non-equivalent points yield valid Kohn surfaces. The only reason for the distinction is to be sure of the origin of the various surfaces.

Now from Figs. III-8 & 9 we see that there are four points where Kohn surfaces cross the [0ζζ] direction. The surface at lowest ζ comes from non-equivalent points, the next from equivalent points, the third from non-equivalent points and the one at largest ζ from equivalent points again. For the first three crossings there are two Kohn surfaces intersecting in the [0ζζ] direction. For the last crossing there is only one

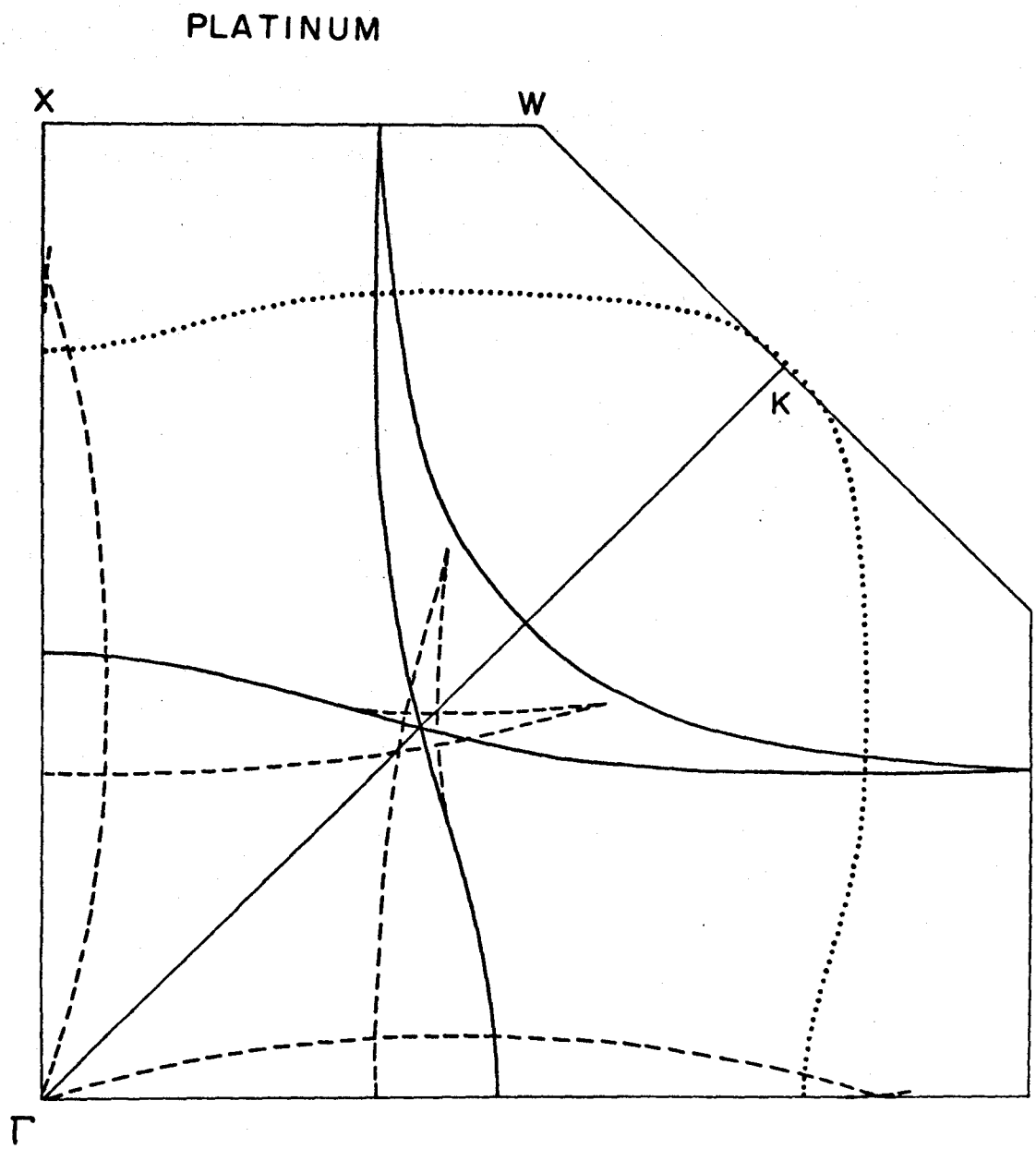

Figure III-8: One quarter of the first Brillouin zone in the (100) plane of Platinum. The heavy solid lines represent possible Kohn surfaces arising from equivalent points on the Fermi surface. The dashed lines represent surfaces arising from non-equivalent points. The dotted line represents the part of the Fermi surface used to obtain these Kohn surfaces.

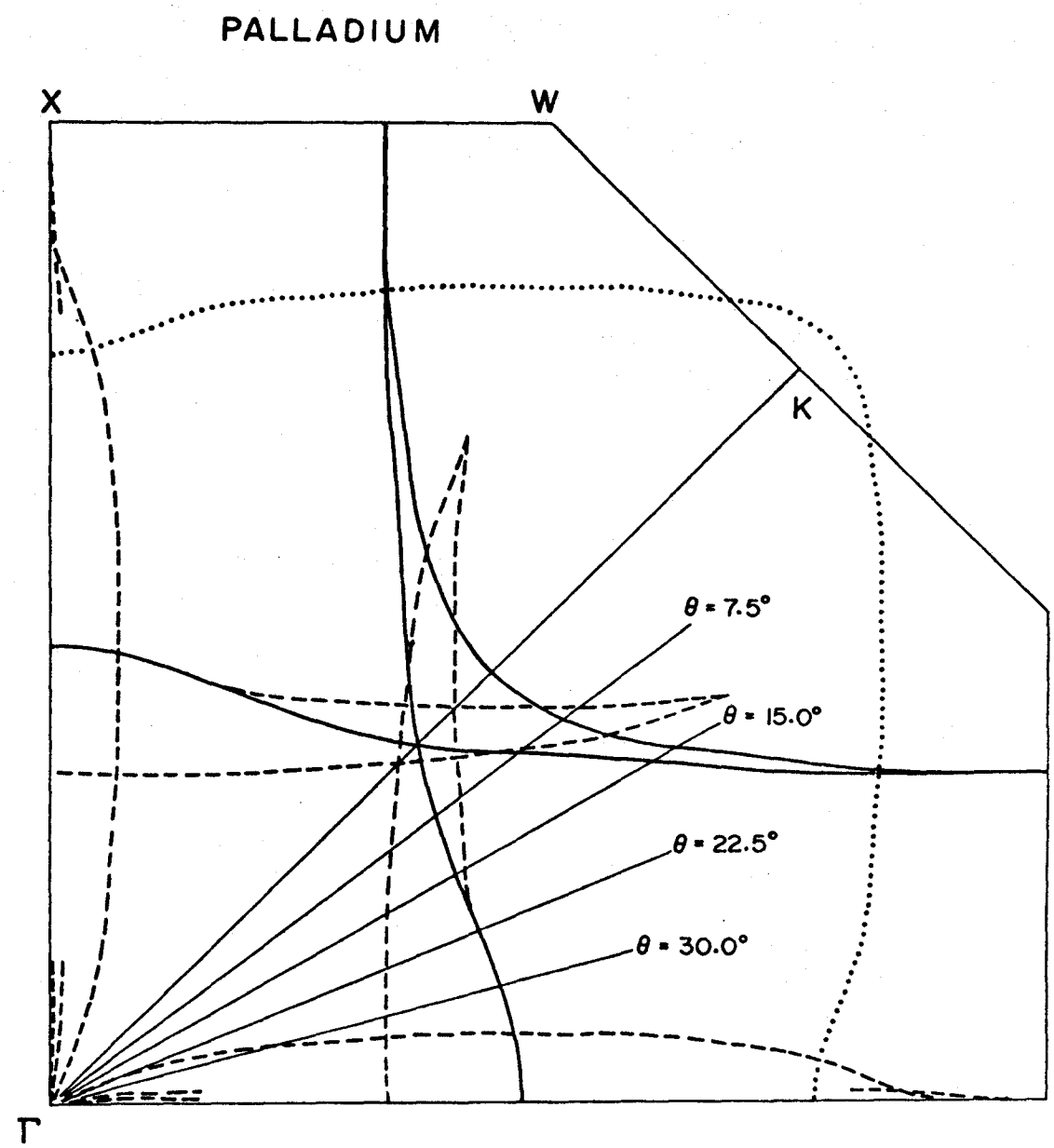

Figure III-9: One quarter of the first Brillouin zone in the (100) plane of Palladium. The heavy solid lines represent possible Kohn surfaces arising from equivalent points on the Fermi surface. The dashed lines represent surfaces arising from non-equivalent points. The dotted line represents the part of the Fermi surface used to obtain these Kohn surfaces.

surface.

The broken and solid arrows of Figs. III-1 and III-3 correspond to the intersections with the [0ζζ] direction of the broken and solid lines in Fig. III-8. In Fig. III-1 we can see that the range of these intersections corresponds to the regions of the anomalies. Moreover we see that in Palladium the Kohn vectors lie in a narrower region than in Platinum. This is rather encouraging since we have already noted that the anomaly in Palladium is somewhat narrower than it is in Platinum. Though the general regions coincide it is difficult to say anything definite about any particular Kohn vector. However it is worth noting that in Pd, at least, the Kohn vectors having the lowest ζ lie just at the point where the rate of change of slope is greatest. The same sort of behaviour is seen in the off-symmetry branches of Palladium in Fig. III-4. Also in these directions we observe that the range of the Kohn vectors spreads out as the angle θ increases. At the same time the anomaly seems to be broadening along the ζ axis.

Now, though this proliferation of Kohn vectors may coincide with the areas of increased slope it does not explain the initial dip in the dispersion curves at $\zeta \simeq 0.35$. Why, forinstance, do the curves not go straight out as far as the first Kohn vector before anything untoward occurs? For this we have not been able to find a suitable explanation. The other point that is difficult to understand is why the anomaly should weaken with increasing temperature. Ordinary Kohn

anomalies (such as those observed in Pb) are not expected to become appreciably less sharp at temperatures as far below the melting points as these are. (The melting points of Palladium and Platinum are respectively 1552 and 1769°C.) It may be that the Fermi surfaces of these metals become less well defined at these temperatures. The disappearance of the anomalies could correspond to an increased uncertainty in the length of the Kohn vectors. At the moment however this is all vain speculation. More experiments are being planned for the future, especially in the off-symmetry directions.

In summary then the anomalies in Palladium and Platinum appear to be real. They do not seem to arise from impurities, magnetic or otherwise. The Kohn effect yields a plausible, if vague, explanation of the behaviour in the T_1 branches. The smaller effects in the other branches can probably be accounted for in the same way. However the theory is not complete inasmuch as it fails to predict the temperature dependence of the anomaly.

TAMAM SHUD

APPENDIX I

Numerical frequency distribution corresponding to Fig II-5

FREQUENCY	.005	.015	.025	.035	.045	.055	.065	.075	.085	.095
0.000	0	1	2	3	5	8	10	14	18	22
.100	27	32	38	44	51	60	67	77	84	93
.200	103	113	123	134	148	158	172	184	200	214
.300	230	259	287	300	306	312	324	347	374	402
.400	431	457	472	481	484	510	533	546	578	619
.500	654	676	702	736	754	781	814	848	875	892
.600	939	979	1001	1033	1070	1117	1161	1180	1206	1253
.700	1303	1352	1398	1428	1469	1510	1554	1575	1614	1677
.800	1739	1789	1831	1885	1948	2000	2051	2097	2102	2188
.900	2251	2287	2347	2414	2491	2573	2603	2649	2725	2800
1.000	2865	2901	2975	3059	3117	3182	3264	3334	3411	3472
1.100	3547	3623	3705	3784	3868	3962	4040	4087	4160	4253
1.200	4354	4447	4515	4617	4705	4802	4884	4988	5087	5147
1.300	5217	5303	5431	5536	5647	5742	5841	5931	6029	6138
1.400	6226	6325	6427	6525	6652	6747	6870	6991	7073	7179
1.500	7274	7361	7474	7604	7714	7826	7947	8079	8163	8286
1.600	8347	8481	8626	8727	8804	8920	9064	9215	9360	9426
1.700	9502	9633	9732	9856	9980	10103	10218	10360	10484	10604
1.800	10714	10836	10963	11069	11153	11280	11431	11567	11720	11853
1.900	11959	12069	12176	12292	12430	12590	12693	12819	12952	13108
2.000	13268	13400	13498	13646	13754	13885	14063	14213	14333	14479
2.100	14654	14802	14925	15044	15199	15347	15497	15659	15820	15991
2.200	16162	16322	16477	16621	16770	16950	17126	17311	17491	17670
2.300	17853	18015	18201	18399	18580	18766	18946	19148	19379	19593
2.400	19785	19993	20207	20422	20654	20886	21118	21363	21610	21859
2.500	22109	22361	22605	22885	23168	23472	23788	24067	24334	24654
2.600	25003	25341	25691	26063	26451	26810	27201	27613	28057	28498
2.700	28979	29502	29967	30509	31101	31722	32433	33144	33850	34666
2.800	35591	36628	37703	39148	40807	42623	46056	52190	54346	49208
2.900	46631	45636	44417	43692	42902	42543	41777	41379	41323	40866
3.000	40373	40097	39723	39505	39391	39349	39109	38826	38491	38373
3.100	38222	38140	38144	37973	37783	37717	37540	37471	37462	37488
3.200	37258	37161	37085	37089	37143	37115	36960	36937	37066	37011
3.300	36909	37090	36946	36452	34752	33754	33086	32469	31945	31492
3.400	31068	30682	30307	29968	29652	29351	29067	28764	28481	28225
3.500	27986	27743	27521	27316	27131	26909	26685	26469	26254	26080
3.600	25902	25743	25558	25447	25250	25021	24844	24738	24644	24419
3.700	24218	24119	24000	23748	23657	23565	23367	23193	23163	22907
3.800	22929	22916	22548	22135	21941	21539	21413	21067	20839	20690
3.900	20479	20159	20008	19878	19685	19429	19241	19102	18952	18802
4.000	18581	18385	18246	18110	17959	17792	17608	17469	17331	17193
4.100	17053	16896	16741	16571	16421	16270	16119	15967	15851	15734
4.200	15566	15417	15254	15094	14952	14839	14693	14526	14368	14219
4.300	14053	13885	13732	13595	13462	13349	13173	12983	12802	12619
4.400	12435	12293	12176	12001	11814	11590	11382	11220	11037	10867
4.500	10705	10554	10324	10062	9845	9694	9551	9333	9086	8922
4.600	8777	8677	8607	8605	8621	8674	8752	8836	8949	9170
4.700	9504	9843	10141	10567	11154	11828	12585	13349	14029	14629
4.800	15292	15982	16544	17108	17667	18440	19198	19910	20628	21383
4.900	22150	23039	23869	24909	25924	27188	29020	31419	31814	32171
5.000	32592	32998	33240	33597	33985	34367	34532	35029	35382	35770
5.100	36001	36243	36584	36993	37402	37632	37845	38211	38483	38853
5.200	39106	39495	39847	40028	40440	40526	40723	41145	41639	41902
5.300	42166	42478	42449	43048	43149	43351	41696	36407	34012	32223
5.400	30331	29040	27728	26773	25687	24689	23861	23022	22193	21490
5.500	20742	20068	19384	18775	18127	17608	16997	16389	15905	15374
5.600	14821	14271	13818	13336	12833	12318	11884	11406	10911	10406
5.700	9954	9530	9037	8512	8029	7494	7034	6508	5860	5254
5.800	4556	3660	2674	2309	1784	1156	92	0	0	0
5.900	0	0	0	0	0	0	0	0	0	0

BIBLIOGRAPHY

R.J. Birgeneau, J. Cordes, G. Dolling and A.D.B. Woods, Phys. Rev. 136, A1359 (1964).

M. Born and T. von Karman, Phys. Zeit. 13, 297 (1912).

L.P. Bouckaert, R. Smoluchowski and E. Wigner, Phys. Rev. 50, 58 (1936).

B.N. Brockhouse and A.T. Stewart, Phys. Rev. 100, 756 (1955); Rev. Mod. Phys. 30, 236 (1958).

B.N. Brockhouse and P.K. Iyengar, Phys. Rev. 111, 747 (1958).

B.N. Brockhouse, in Inelastic Scattering of Neutrons in Solids and Liquids,p. 113, (International Atomic Energy Agency, Vienna, 1961).

B.N. Brockhouse, T. Arase, S. Caglioti, K.R. Rao and A.D.B. Woods, Phys. Rev. 128 , 1099 (1962).

B.N. Brockhouse, S. Hautecler and H. Stiller, in The Interaction of Radiation with Solids,p.580,edited by R. Strumane, J. Nohoul, R. Gevers and S. Amelinckx, (North-Holland Publishing Co., Amsterdam, 1964)

B.N. Brockhouse, E.D. Hallman and S.C. Ng, in Magnetic and Inelastic Scattering of Neutrons by Metals, edited by T.J. Rowland and P.A. Beck (Gordon and Breach Science Publishers Inc., New York,1967)

B.N. Brockhouse, G.A. deWit, E.D. Hallman and J.M. Rowe, International Atomic Energy Agency Symposium on Neutron Inelastic Scattering, Copenhagen, May, 1968.

R.S. Carter, H. Palevsky and D.J. Hughes, Phys. Rev. 106, 1168 (1957)

W. Cochran, in Inelastic Scattering of Neutrons, Vol. I, p.3, (International Atomic Energy Agency, Vienna, 1965).

H. Cole and B.E. Warren, J. App. Phys. 23, 335 (1952).

H. Curien, Acta Cryst. 5, 393 (1952).

P. Debye, Ann. d. Phys. 39, 789 (1912).

A. Einstein, Ann. d. Phys. 22, 180 (1907).

E. Fermi, Ric. Scient. 7, 13 (1936).

A.J.E. Foreman and W.M. Lomer, Proc. Phys. Soc. (London) B70, 1143 (1957).

G. Gilat and L.J. Raubenheimer, Phys. Rev. 144, 390 (1966).

R. Hultgren, R.L. Orr, P.D. Anderson and K.K. Kelley, Selected Values of Thermodynamic Properties of Metals and Alloys, (John Wiley and sons Inc., New York, 1963)

P.K. Iyengar, in Thermal Neutron Scattering, p.98, edited by P.A. Egelstaff,(Academic Press, New York,1965).

E.H. Jacobsen, Phys. Rev. 97, 654 (1955).

W. Kohn, Phys. Rev. Letters, 2,393 (1959).

O. Krogh Andersen and A.R. Mackintosh, Solid State Commun. 6, 285 (1968).

J. Laval, Bull. Soc. Franc. Mineral 1, 64 (1941).

R.E. Macfarlane and J.A. Rayne, Phys Letters 18, 91 (1965)

A.P. Miiller and B.N. Brockhouse,Phys. Rev. Letters 20,15 798 (1968).

A.P. Miiller, Ph.D. Thesis, McMaster University (1969) (unpublished)

Ph. Olmer, Acta Cryst. 1, 57 (1948); Bull. Soc. Franc. Mineral 71,144 (1948).

R. Orlich and W. Drexel, International Atomic Energy Agency Symposium on Neutron Inelastic Scattering, p.203, Copenhagen, May, 1968.

G. Placzek and L. Van Hove, Phys. Rev. 93, 1207 (1954).

J.M. Rowe, Ph.D. Thesis, McMaster University, (1966) (unpublished)

L.I. Schiff, Quantum Mechanics, (third edition), (McGraw Hill Inc., New York, 1968).

A. Sommerfeld, Z. Physik 47, 1 (1928).

E.C. Svensson, B.N. Brockhouse and J.M. Rowe, Solid State Commun. 3, 245 (1965).

L. Van Hove, Phys. Rev. 95, 249 (1954).

C.B. Walker, Phys. Rev. 103, 547 (1956).

A.D.B. Woods, B.N. Brockhouse, R.H. March, A.T. Stewart, and R. Bowers, Phys. Rev. 128, 1112 (1962)

J.M. Ziman, Adv. in Phys. 13, 89 (1964).